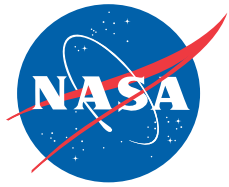


NASA/TM-2006-213673



Design and Flight Evaluation of a New Force-Based Flow Angle Probe

*Stephen Corda and Michael Jacob Vachon
NASA Dryden Flight Research Center
Edwards, California*

February 2006

NASA STI Program ... in Profile

Since its founding, NASA has been dedicated to the advancement of aeronautics and space science. The NASA scientific and technical information (STI) program plays a key part in helping NASA maintain this important role.

The NASA STI program is operated under the auspices of the Agency Chief Information Officer. It collects, organizes, provides for archiving, and disseminates NASA's STI. The NASA STI program provides access to the NASA Aeronautics and Space Database and its public interface, the NASA Technical Report Server, thus providing one of the largest collections of aeronautical and space science STI in the world. Results are published in both non-NASA channels and by NASA in the NASA STI Report Series, which includes the following report types:

- **TECHNICAL PUBLICATION.** Reports of completed research or a major significant phase of research that present the results of NASA programs and include extensive data or theoretical analysis. Includes compilations of significant scientific and technical data and information deemed to be of continuing reference value. NASA counterpart of peer-reviewed formal professional papers but has less stringent limitations on manuscript length and extent of graphic presentations.
- **TECHNICAL MEMORANDUM.** Scientific and technical findings that are preliminary or of specialized interest, e.g., quick release reports, working papers, and bibliographies that contain minimal annotation. Does not contain extensive analysis.
- **CONTRACTOR REPORT.** Scientific and technical findings by NASA-sponsored contractors and grantees.

- **CONFERENCE PUBLICATION.** Collected papers from scientific and technical conferences, symposia, seminars, or other meetings sponsored or cosponsored by NASA.
- **SPECIAL PUBLICATION.** Scientific, technical, or historical information from NASA programs, projects, and missions, often concerned with subjects having substantial public interest.
- **TECHNICAL TRANSLATION.** English-language translations of foreign scientific and technical material pertinent to NASA's mission.

Specialized services also include creating custom thesauri, building customized databases, and organizing and publishing research results.

For more information about the NASA STI program, see the following:

Access the NASA STI program home page at <http://www.sti.nasa.gov>.

- E-mail your question via the Internet to help@sti.nasa.gov.
- Fax your question to the NASA STI Help Desk at (301) 621-0134.
- Phone the NASA STI Help Desk at (301) 621-0390.
- Write to:
NASA STI Help Desk
NASA Center for AeroSpace Information
7121 Standard Drive
Hanover, MD 21076-1320

NASA/TM-2006-213673



Design and Flight Evaluation of a New Force-Based Flow Angle Probe

*Stephen Corda and Michael Jacob Vachon
NASA Dryden Flight Research Center
Edwards, California*

National Aeronautics and
Space Administration

Dryden Flight Research Center
Edwards, California 93523-0273

February 2006

NOTICE

Use of trade names or names of manufacturers in this document does not constitute an official endorsement of such products or manufacturers, either expressed or implied, by the National Aeronautics and Space Administration.

Available from the following:

NASA Center for AeroSpace Information
7121 Standard Drive
Hanover, MD 21076-1320
(301) 621-0390

National Technical Information Service
5285 Port Royal Road
Springfield, VA 22161-2171
(703) 605-6000

ABSTRACT

A novel force-based flow angle probe was designed and flight tested on the NASA F-15B Research Testbed aircraft at NASA Dryden Flight Research Center. The prototype flow angle probe is a small, aerodynamic fin that has no moving parts. Forces on the prototype flow angle probe are measured with strain gages and correlated with the local flow angle. The flow angle probe may provide greater simplicity, greater robustness, and better access to flow measurements in confined areas relative to conventional moving vane-type flow angle probes. Flight test data were obtained at subsonic, transonic, and supersonic Mach numbers to a maximum of Mach 1.70. Flight conditions included takeoff, landing, straight and level flight, flight at higher aircraft angles of attack, and flight at elevated g -loadings. Flight test maneuvers included angle-of-attack and angle-of-sideslip sweeps. The flow angle probe-derived flow angles are compared with those obtained with a conventional moving vane probe. The flight tests validated the feasibility of a force-based flow angle measurement system.

NOMENCLATURE

AFTF	Aerodynamic Flight Test Fixture
b	width of prototype FLAP, in.
C	distance from neutral axis to furthest point on the part, in.
C_N	normal force coefficient
CG	center of gravity
CAS	control augmentation system
CLIP	Centerline Instrumented Pylon
FLAP	flow angle probe
g	acceleration due to gravity, ft/s ²
mV	millivolt
N	normal force, lbf
NACA	National Advisory Committee for Aeronautics
NASA	National Aeronautics and Space Administration
PFTF	Propulsion Flight Test Fixture
q	dynamic pressure, lbf/ft ²
S	FLAP reference area, ft ²
T	temperature, °F
α	angle of attack or local flow angle, deg
β	angle of sideslip, deg

INTRODUCTION

The measurement of local flow angle is important in many external and internal flow applications, including the flight testing of aircraft. A novel force-based flow angle measurement instrument, the flow angle probe (FLAP), was developed, flight tested, and patented (fig. 1 and ref. 1). The prototype FLAP is a small, aerodynamic fin that measures forces correlated to the local flow angle. Having no moving parts, the FLAP may provide greater simplicity, greater robustness, and increased measurement access relative to conventional moving vane-type flow angle probes.

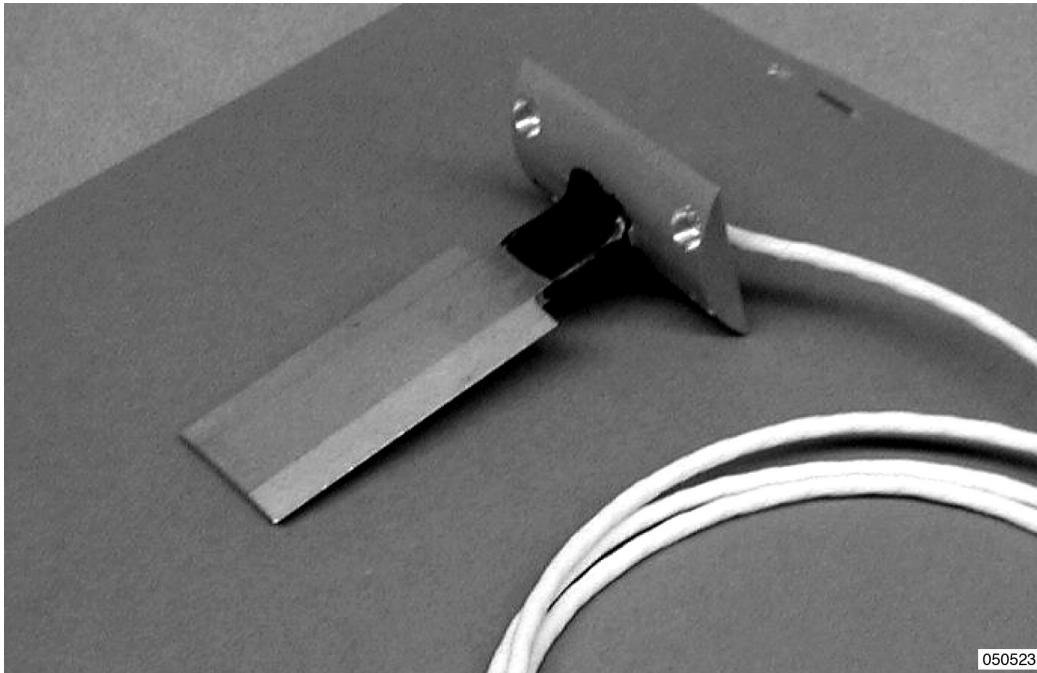


Figure 1. Force-based flow angle probe (U.S. Patent No. 6,526,821).

The FLAP force measurement is made using various techniques, encompassing those that use conventional, electrical resistance strain gages as well as those that apply advanced, optical fiber technology. This paper reports on the design and testing of an electrical resistance strain gage FLAP. Fiber optic technology allows for the construction of a much smaller force-based instrument, permitting flow angle measurement in confined regions that may be less accessible for direct measurement. This technology may also enable the “tufting” of a surface with miniature FLAPs, capable of quantitative flow angle measurement, similar to attaching yarn tufts for qualitative measurements. A conceivable likelihood exists to “weave” optical fibers into a surface, thus making the surface itself a flow angle sensing “skin.” A fiber optic-based FLAP has already been designed and constructed, and this FLAP is expected to be flight tested in the near future.

Flight testing of the prototype FLAP was performed on the NASA F-15B Research Testbed aircraft at NASA Dryden Flight Research Center (Edwards, California). The FLAP was attached to a National Advisory Committee for Aeronautics (NACA) airdata boom on the leading edge of the F-15B Aerodynamic Flight Test Fixture (AFTF) (ref. 2), a fin-like structure that is hung

underneath the aircraft fuselage. The FLAP flight test data were collected at subsonic, transonic, and supersonic speeds to a maximum of Mach 1.70 and altitudes to a maximum of 45,000 ft (13,716 m). The FLAP response was also evaluated for local flow angles of attack approaching stall and elevated g -loadings. The FLAP-derived local flow angles were compared to those obtained using a conventional moving vane flow angle probe (fig. 2).

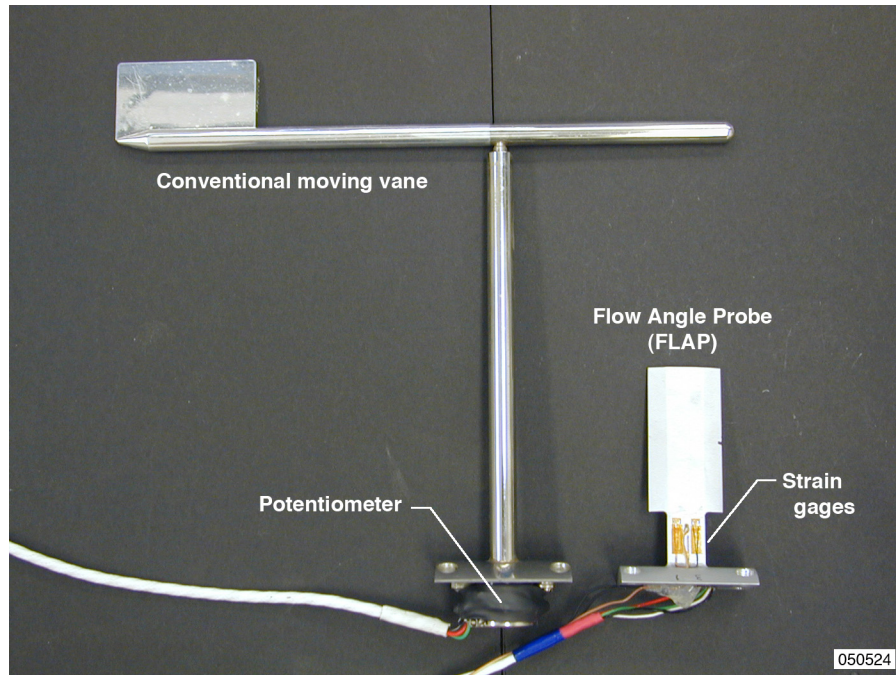


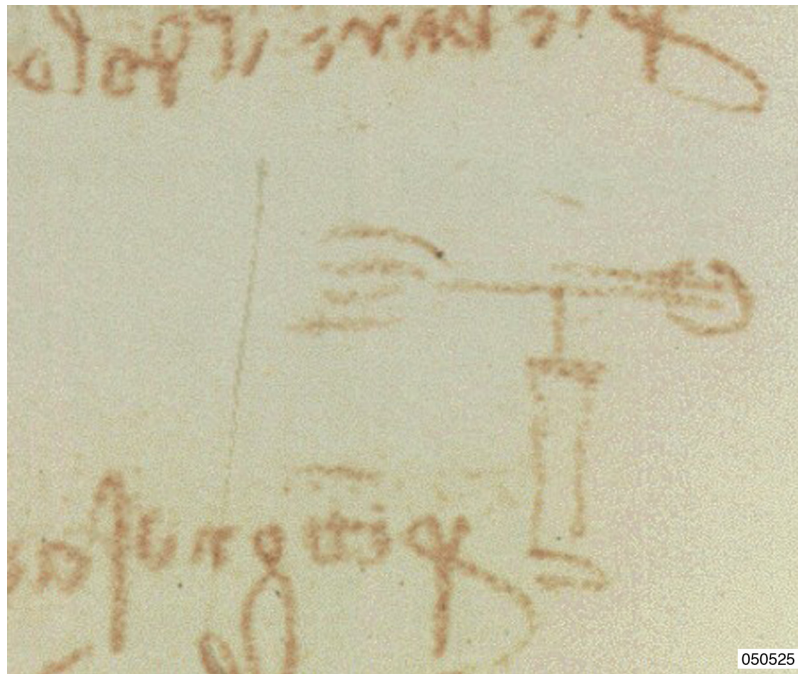
Figure 2. Conventional moving vane and flow angle probe.

BACKGROUND

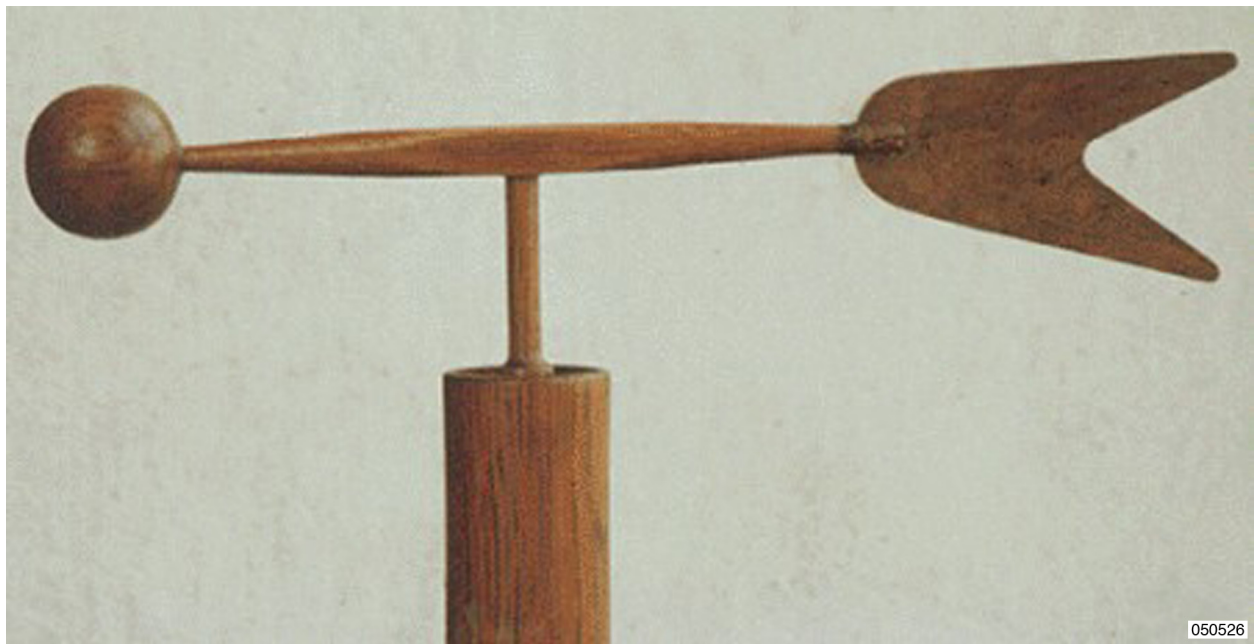
This section provides a brief review of the development and state-of-the-art of flow angle measurement, encompassing conventional moving vane-type devices, pressure-based devices, and force-based techniques. The paper also discusses other qualitative flow angle measurement techniques.

Early Innovations in Flow Angle Measurement

A flight instrument designed to indicate the wind direction dates back to the 15th century. Leonardo da Vinci designed the “anemoscope” (figs. 3(a) and 3(b)) between 1483 and 1486. He deemed this device as “necessary for human flight by providing insight into the character of the wind” (ref. 3). The anemoscope is a moving vane-type device that is similar in appearance and operation to modern wind direction vanes.



(a). Original drawing of anemoscope from Leonardo da Vinci.



(b). Model of anemoscope in National Museum of Science and Technology, Milan, Italy.

Figure 3. Anemoscope illustrations (ref. 3).

The Wright brothers also deserve credit for another significant flow angle measurement device. The original Wright Flyer (fig. 4(a)) was intentionally designed to be unstable in pitch, roll, and yaw to enhance maneuverability; however, this unstable flying quality made the Wright Flyer difficult to fly. After their successful first flights in 1903, the Wright brothers invented an angle-of-attack sensor for their “automatic stabilizer” to decrease pilot workload (refs. 4 and 5). They flight tested and improved this innovation during numerous glider flights at Kitty Hawk, North Carolina, between 1905 and 1908.

Figure 4(b) shows the arrangement of the automatic stabilizer on the Wright Flyer. The flow angle sensing component of the system was an angle-of-attack vane that aligned itself with the local flow. Several vane geometries were investigated including a simple flat plate and trailing-type fin counterweighted with a spherical mass. The response of the angle-of-attack vane was used to “automatically” position the aircraft elevator using pneumatic power from a compressed air tank and actuating piston. The pilot set the angle-of-attack limits using a hand control. In addition to incorporating an innovative flow angle measurement device, the automatic stabilizer may also be the first example of a flight control augmentation system (CAS) with feedback.

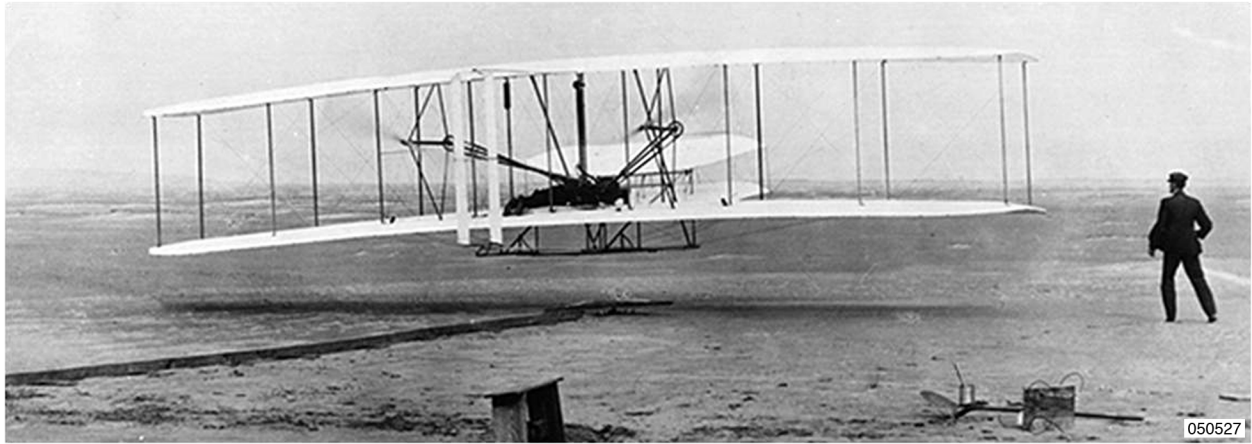
State-of-the-Art, Conventional Flow Angle Measurement

State-of-the-art in-flight flow angle measurements include the differential pressure probe (fig. 5(a)) and the mechanical pivoted vane (fig. 5(b)). The mechanical pivoted vane is a “weather vane” type device. Typically, the vane connects to a potentiometer or servo mechanism. The pressure-based device detects the relative airflow by measuring the differential pressure through ports or slots. This class of flow angle detection also includes flush airdata systems (FADS), where pressure ports are typically distributed around the nose of a flight vehicle. Both the pressure-based and moving vane systems, however, may be susceptible to problems with contamination or blockage.

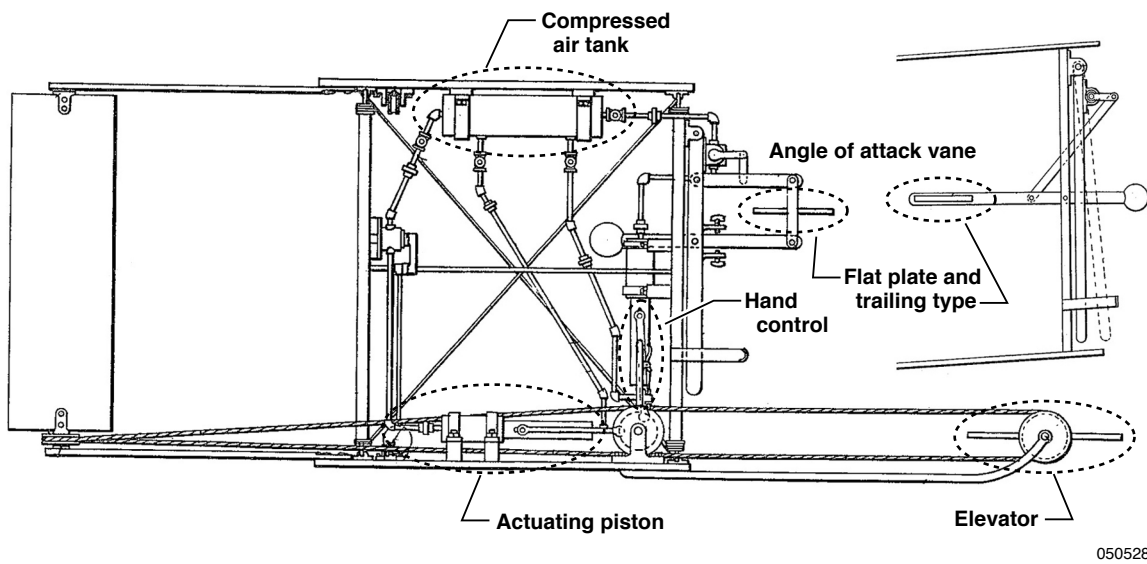
Other flow angle measurement techniques available today involve flow visualization using tufts, oil, smoke, dye, etc. These techniques typically provide qualitative flow angle information. The application of these techniques is not usually suitable for use on a continual basis, but is more suitable for one-time use of limited duration.

Force-Based Flow Angle Measurement

Perhaps the first force-based flow angle measurement device was developed not for aviation, but rather for marine applications. In 1967, Tourmen (ref. 6) invented a water wave direction device for coastal engineering studies (figs. 6(a) and 6(b)). Tourmen’s device consists of a sphere mounted on a vertical rod that was placed on the sea floor. The drag on the sphere, because of wave action, bends the rod and is measured by a strain gage bridge at the base of the rod. The constant current direction was filtered to measure the wave directions only.

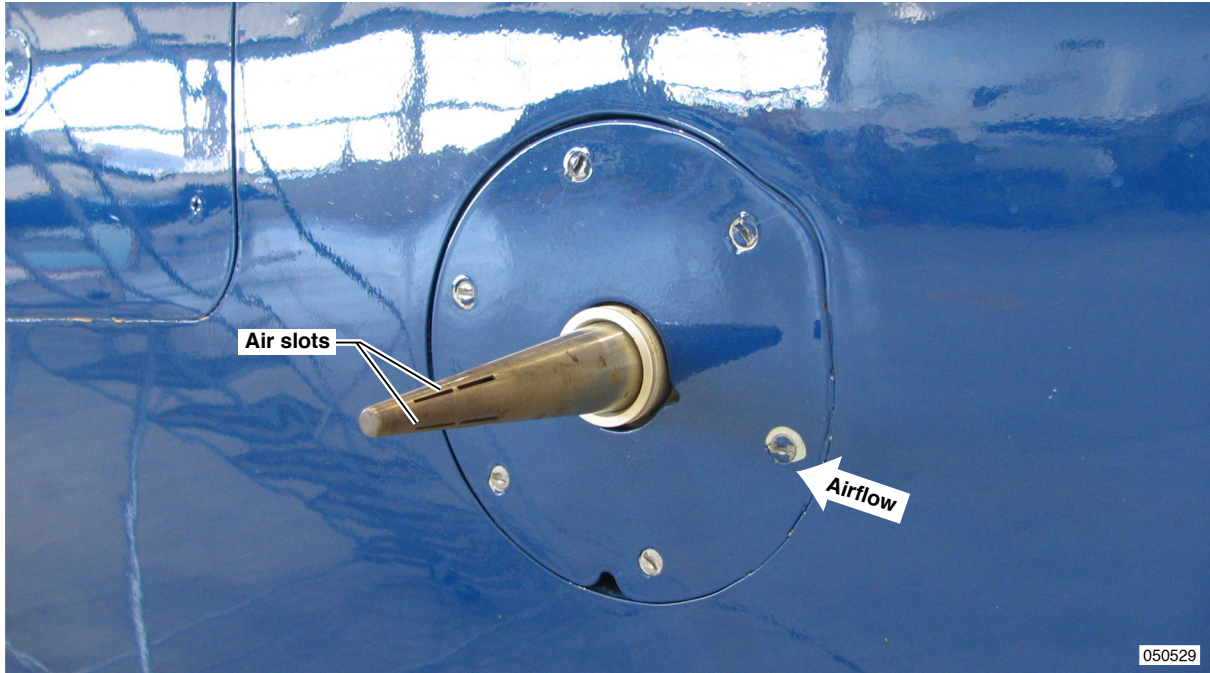


(a). Wright Flyer, 1903 (Library of Congress, LC-USZ62-6166-A).

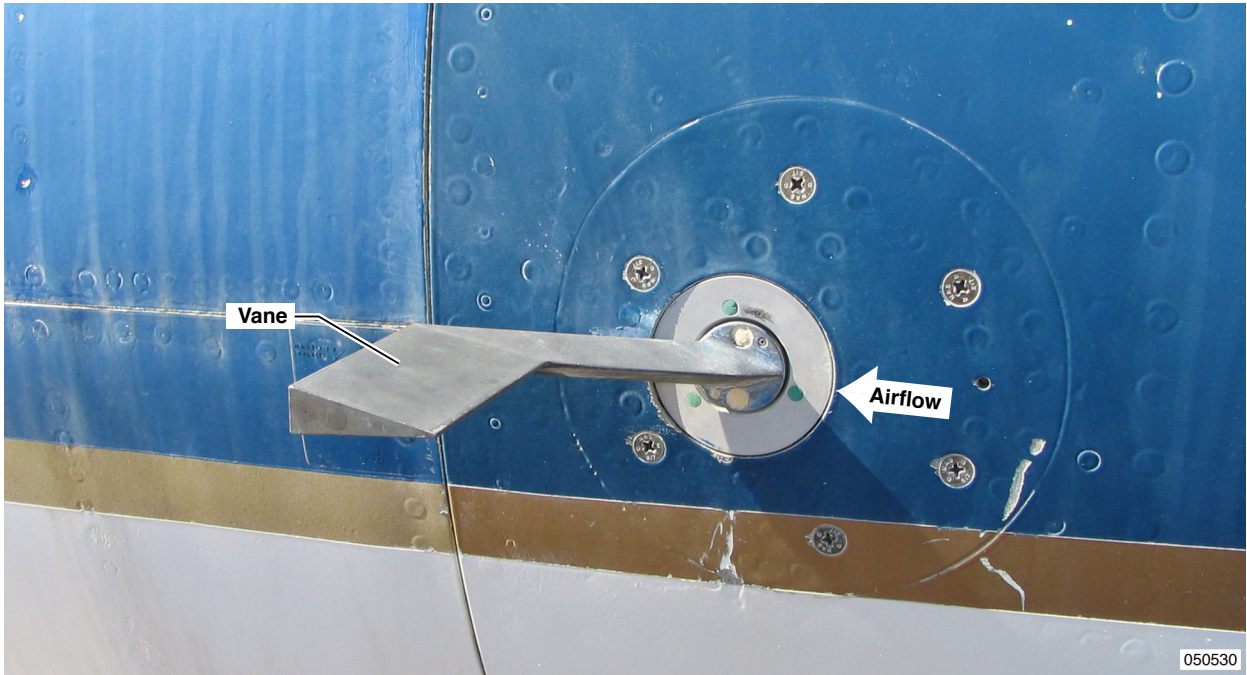


(b). Wright Flyer automatic stabilizer, 1908 (U.S. Patent 1,075,533).

Figure 4. Wright Flyer illustrations (ref. 4).

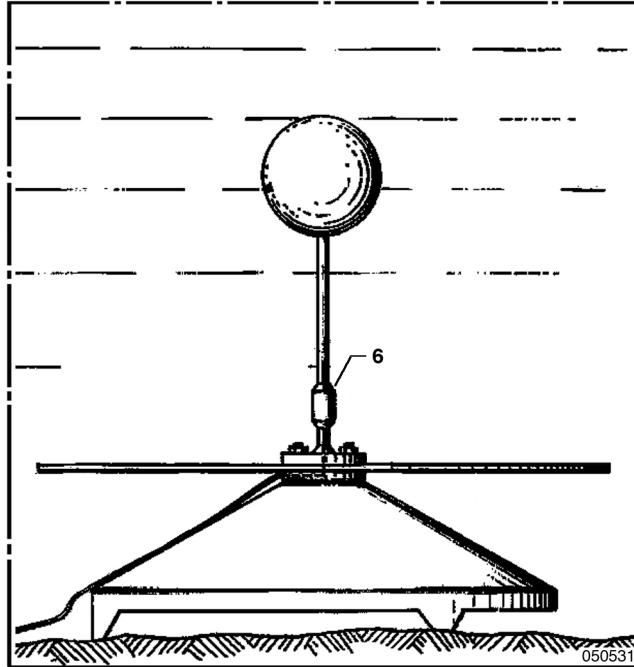


(a). Differential pressure probe.

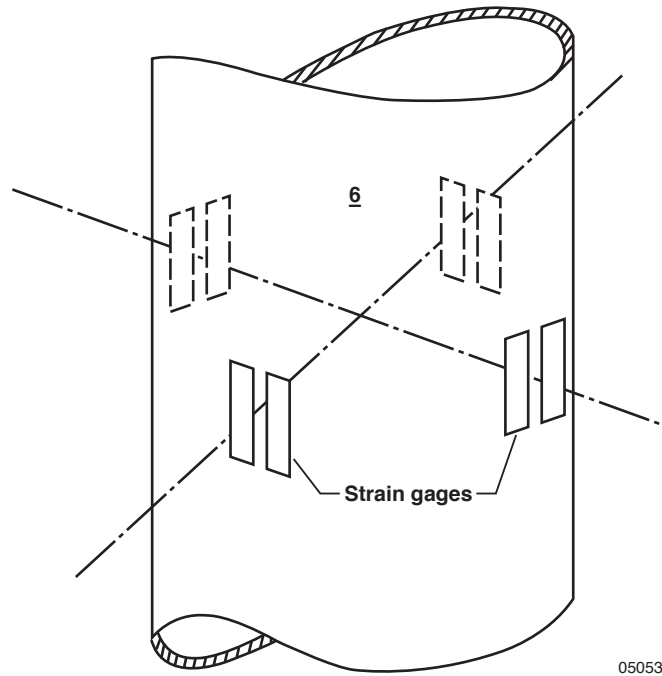


(b). Mechanical pivoted vane.

Figure 5. Conventional flow angle measurement devices.



(a). Water wave direction device.



(b). Strain gage bridge on Tourmen water wave direction device.

Figure 6. Tourmen water wave direction device (ref. 6).

In 1992, Gerardi developed an omnidirectional aerodynamic sensor (ref. 7) using a rod-sphere geometry and strain gages (figs. 7(a) and 7(b)) similar to Tourmen's water wave device. The strain gages measured the force on the sphere and were calibrated to the flow angle. Based on the past quantitative and qualitative flow angle measurement capabilities, the need arose to develop a device with the following features:

- Capability to obtain flow angle from the measurement of aerodynamic forces.
- Force measurement using conventional strain gages or newer fiber optic-based techniques.
- Simplicity and durability in operation, i.e., no moving parts.
- Potential for fabrication of a very small, nonobtrusive sensor.
- Ability to make quantitative, detailed flow measurements of the local flow.
- Ability to obtain flow angles in subsonic, transonic, and supersonic flow.

AIRCRAFT AND FLIGHT TEST FIXTURE DESCRIPTIONS

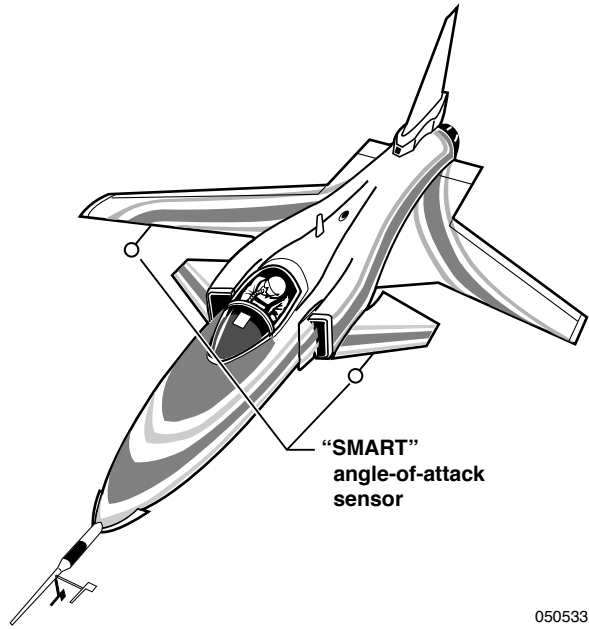
This portion of the paper provides a further discussion of the aircraft and flight test fixture. Several sections deal with aircraft, AFTF, and conventional moving vane descriptions as well as instrumentation.

Aircraft Description

The F-15B aircraft (fig. 8) is a two-seat fighter/trainer version of the F-15A high performance, air-superiority fighter manufactured by McDonnell Aircraft Company (now The Boeing Company, St. Louis, Missouri). The airplane has a length of 63.7 ft (19.40 m), excluding the airdata noseboom; wingspan of 42.8 ft (13.05 m); and height of 18.7 ft (5.70 m). The aircraft configuration includes a shoulder-mounted main wing with a modified delta shape, twin vertical tails, all-moving horizontal stabilators, two engines mounted close together in the aft fuselage, and elevated cockpit to enhance visibility. A hydromechanical system and an electrical CAS control the primary flight control surfaces.

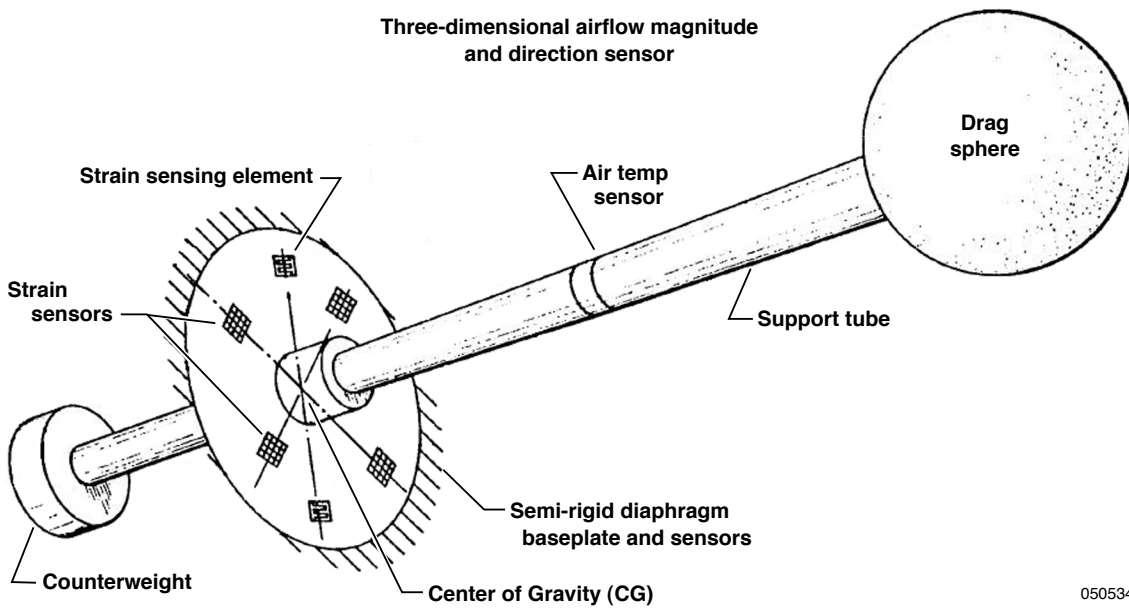
Two Pratt & Whitney (West Palm Beach, Florida) F100-PW-100 turbofan engines power the NASA F-15B aircraft. Each engine produces an uninstalled, sea level static thrust of approximately 23,500 lbf (104,533 N) in full afterburner. The aircraft is capable of dash speeds in excess of Mach 2.00 at altitudes of 40,000 ft (12,192 m) to 60,000 ft (18,288 m). The aircraft has a fully fueled takeoff weight of approximately 42,000 lb (19,051 kg) and a landing weight of approximately 32,000 lb (14,515 kg). The aircraft also has aerial refueling capability for extended-duration research missions.

The NASA F-15B aircraft was modified from its role as an air-superiority fighter into a supersonic research testbed. These modifications include the removal of radar and weapons systems as well as the installation of research systems for instrumentation, digital data recording, telemetry, in-flight video, and global positioning system (GPS) navigation. A significant feature of the research capability of the aircraft is the ability to carry large experiment test fixtures underneath the aircraft on a fuselage centerline pylon.



050533

(a). Gerardi omnidirectional aerodynamic sensor installed on aircraft.



050534

(b). Sensor.

Figure 7. Gerardi omnidirectional aerodynamic sensor (ref. 7).

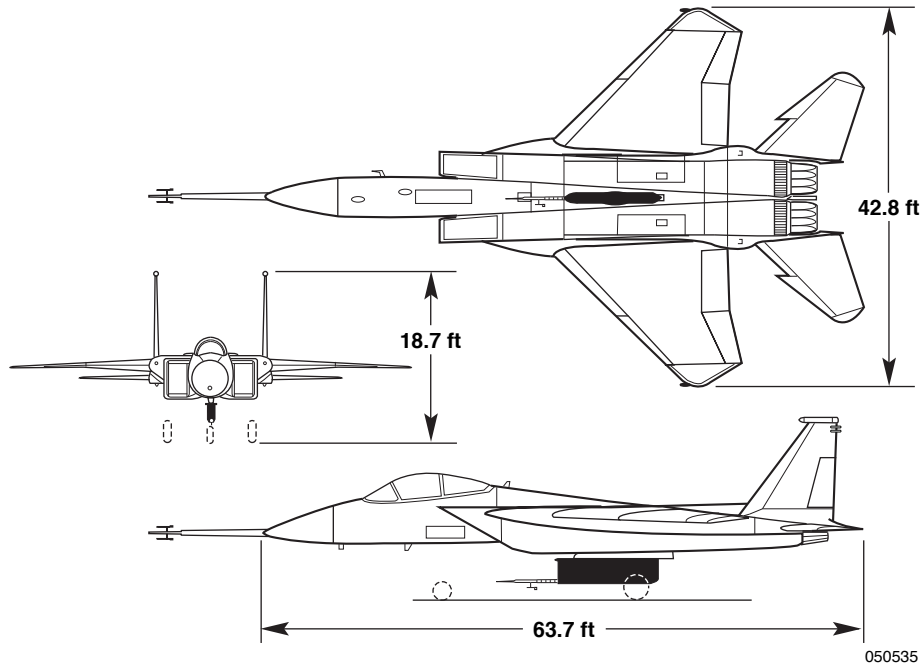


Figure 8. NASA F-15B Research Testbed aircraft, shown with Aerodynamic Flight Test Fixture and airdata boom.

Aerodynamic Flight Test Fixture Description

The Aerodynamic Flight Test Fixture (AFTF, previously called the Flight Test Fixture-II) is the second generation AFTF that has replaced the first flight test fixture, flown on a NASA F-104 aircraft (refs. 2 and 8). The AFTF is a low aspect ratio, rectangular fin shape that is mounted underneath the aircraft on the fuselage centerline pylon (fig. 8). It has an elliptical leading edge nose section and a blunt, squared-off base. Constructed of all composite materials, the AFTF has a modular structure with four upper and four lower internal bays. The bays are accessible through removable side panels. The AFTF has a length of 107.0 in. (2.72 m), height of 32.0 in. (0.8128 m), and width of 8.0 in. (0.2032 m). The typical AFTF weight with its instrumentation system installed is between 450 lb (204 kg) and 600 lb (272 kg).

The AFTF complements the current inventory of NASA F-15B experiment flight test fixtures, the Propulsion Flight Test Fixture (PFTF) (refs. 9 and 10) and the Centerline Instrumented Pylon (CLIP). The PFTF is designed to carry advanced propulsion experiments, and the CLIP is designed to accommodate larger span models underneath the aircraft.

Instrumentation

Standard NACA airdata booms are mounted on the F-15B aircraft nose and on the AFTF leading edge. Each airdata boom measures the local total pressure, static pressure, angle of attack,

and angle of sideslip. Each airdata boom contains two sets of static pressure ports separated by 0.75 in. (19.05 mm). The pressure measurements from the two sets of ports were averaged to obtain Mach number and altitude. The data were digitally recorded onboard the aircraft and telemetered to ground-based recorders and control room displays in real time. Data sample rates for the aircraft and AFTF airdata booms were 50 samples per s and 800 samples per s, respectively.

Conventional Moving Vane Description

Conventional moving flow angle vanes (for measurement of angle of attack and angle of sideslip) are mounted downstream of the static pressure ports of each airdata boom. The moving vane swivels about a 0.375 in. (9.525 mm) diameter shaft that extends approximately 6 in. (152.4 mm) from the probe mounting pad. The moving vane is comprised of a 9.2 in. (233.68 mm) long cylindrical rod with a 0.313 in. (7.950 mm) diameter, hemi-spherical nose. A flat plate fin with a 2 in. (50.8 mm) length and 1.3 in. (33.02 mm) height is mounted on the rod trailing edge. A potentiometer behind the probe mounting pad senses the rotational motion of the moving vane. The complete moving vane probe has a total weight of approximately 7 oz (198 gm) (fig. 2).

FLOW ANGLE PROBE DESCRIPTION AND DESIGN

This paper also includes a description of the FLAP and design. The following sections elaborate upon this design as well as present significant correlations.

Flow Angle Probe Geometry

The initial FLAP design is a 3-in. (76.2-mm) long probe consisting of a mounting base, a strut section, and an aerodynamically shaped, low aspect ratio fin (figs. 1 and 9). The prototype FLAP is constructed of 2024-T351 aluminum. The fin has a length of 2 in. (50.8 mm), width of 1 in. (25.4 mm), and thickness of 0.125 in. (3.175 mm). The fin has a rectangular planform with a symmetric double wedge cross section with a flat surface in the center section. The fin leading and trailing edges have half wedge angles of 12 deg.

Electrical resistance strain gages measure forces on the FLAP. Four strain gages are mounted on the FLAP strut section, two on the upper surface and two on the lower surface. The gages connect to form a full Wheatstone bridge configured as a bending bridge.

Flow Angle Probe Theory of Operation

Figure 10 graphically shows the theory of how the flow angle is obtained from the FLAP force measurement. Two predetermined correlations are required—a correlation between the strain gage output, typically in millivolts, mV, and the force, N , as a function of temperature, T ; and a correlation between the force, N , and the flow angle, α , as a function of dynamic pressure, q . Since the correlations require that the static temperature and dynamic pressure are known, requirements encompass measurements of the static temperature, static pressure, and total pressure.

As figure 10 shows, the flow exerts a force, N , on the FLAP that is measured as a strain by the strain gages. Knowing the temperature, T , and strain gage output, the force, N , is obtained using the static loads correlation. Knowing the force, N , and dynamic pressure, q , the flow angle is obtained using the force-to-flow angle correlation.

For the prototype FLAP, a static loads test that was performed inside a temperature-controlled chamber was used to obtain the mV-to-force calibration. The force-to-flow angle correlation, however, is obtained using various techniques such as analytical models, wind-tunnel testing, and computational fluid dynamics. For the prototype FLAP, a simple analytical model was used to obtain the force-to-flow angle correlation.

Flow Angle Probe Force-to-Flow Angle Correlation

As discussed previously, the prototype FLAP force-to-flow angle correlation was obtained using a simple analytical model. Despite the simplistic nature of this correlation, the results obtained were much better than anticipated. Additionally, a wind-tunnel-based correlation is planned to improve the accuracy of the FLAP.

For the simple analytical model, the FLAP normal force is calculated using flat plate theory (ref. 11). For this analysis, the center of pressure is assumed to be the centroid of the FLAP planform area, not including the area of the mounting base. Equation (1) defines the flat plate normal force coefficient, C_N , as a function of the angle of attack or flow angle, α .

$$C_N = \frac{1}{0.222 + \frac{0.283}{\sin \alpha}} \quad (1)$$

Equation (2) gives the normal force, N , for a particular dynamic pressure, q , and FLAP planform area, S . The dynamic pressure, q , is calculated using the measured static and total pressures.

$$N = q \cdot S \cdot C_N \quad (2)$$

Equation (3) explicitly gives the force-to-flow angle correlation by substituting equation (2) into equation (1).

$$N = \frac{q \cdot S}{0.222 + \frac{0.283}{\sin \alpha}} \quad (3)$$

Flow Angle Probe Strain-to-Force Correlation

Static loading of the FLAP was performed to obtain the strain-to-force correlation. Static weights were applied to the FLAP in 1-lbf increments to a maximum static load of 30 lbf (133 N). Data were obtained in a temperature-controlled chamber at a minimum and maximum air temperature of $-65\text{ }^{\circ}\text{F}$ (219.3 K) and $160\text{ }^{\circ}\text{F}$ (344.3 K), respectively. During data collection at discrete temperatures, the air temperature was held constant for approximately 30 min for temperature stabilization.

Figure 11 shows the FLAP strain-to-normal force correlation obtained as a function of temperature. The FLAP strain-to-force correlation is linear with a maximum strain of approximately $3,600\text{ }\mu\text{in./in.}$ ($3,600\text{ }\mu\text{m/m}$) at the maximum load of 30 lbf (133 N). For reference, the strain yield limit for aluminum is $4,500\text{ }\mu\text{in./in.}$ ($4,500\text{ }\mu\text{m/m}$).

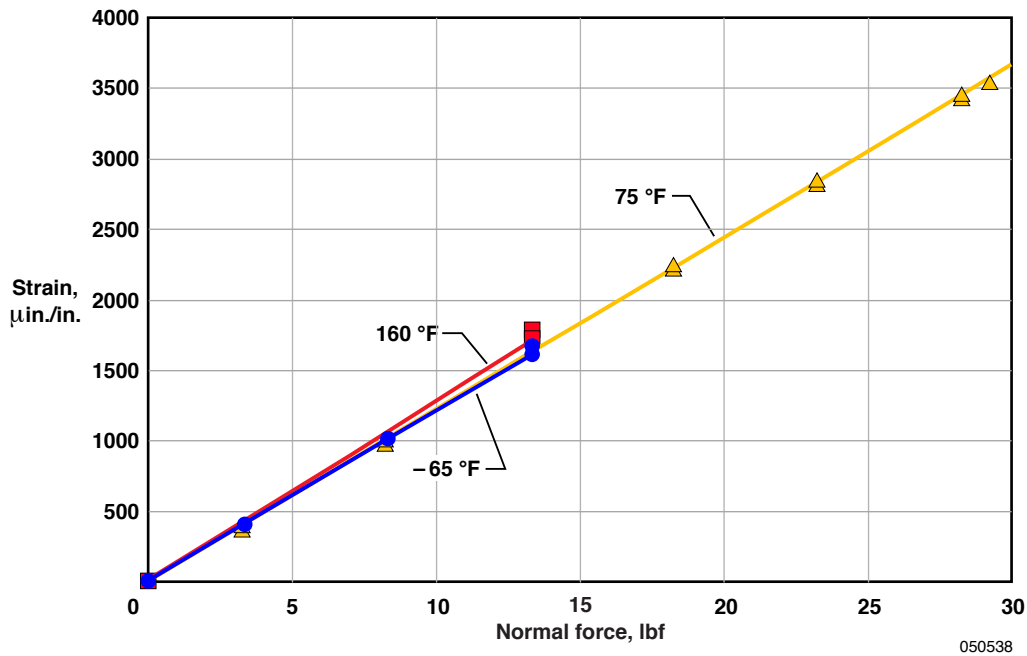


Figure 11. Flow angle probe strain-to-normal force calibration as function of temperature.

The symmetry of the strain-to-force calibration was verified by loading the upper and lower planform surfaces of the FLAP in separate tests. Simply “flipping” the FLAP over and loading the fin accomplished this verification.

Thermal effects on the correlation were small. When loaded to 13 lbf (58.8 N), the FLAP output strain varies linearly from $120\text{ }\mu\text{in./in./lbf}$ ($27\text{ }\mu\text{m/m/N}$) at $-65\text{ }^{\circ}\text{F}$ (219.3 K) to $129\text{ }\mu\text{in./in./lbf}$ ($29\text{ }\mu\text{m/m/N}$) at $160\text{ }^{\circ}\text{F}$ (344.3 K) (fig. 11). This variation in output because of temperature results in less than 1/100,000 of a percent change in the calculated flow angle.

Flow Angle Probe Structural Analysis

The performance of structural analysis of the FLAP verified its structural integrity. A solid model of the FLAP was analyzed using the COSMOSWorks™ (Structural Research and Analysis Corporation, a division of SolidWorks Corporation, Concord, Massachusetts) finite element analysis utility in the SolidWorks® (SolidWorks Corporation, Concord, Massachusetts) software package. Flat plate theory was used to estimate the forces on upper and lower surfaces of the FLAP. An assumption was made that the pressure forces acted on the FLAP planform with the FLAP base held rigidly fixed at its screw holes.

Since the largest FLAP load was expected from the static load ground test, this loading was used as a worst case for the finite element analysis. The static load test setup used a fixture that had a 0.5 in. (12.7 mm) diameter footpad that rested on the FLAP planform. The resultant load placed on the FLAP acted across this footpad area. In the finite element analysis, the maximum flight predicted load of 30 lbf (133 N) was applied on the simulated footpad area. The finite element analysis showed that the FLAP structure has a factor of safety (FS) of 1.5.

FLIGHT TEST DESCRIPTION

This section provides a concise description of flight test. The section includes discussions of flight test configuration as well as flight test conditions.

Flight Test Configuration

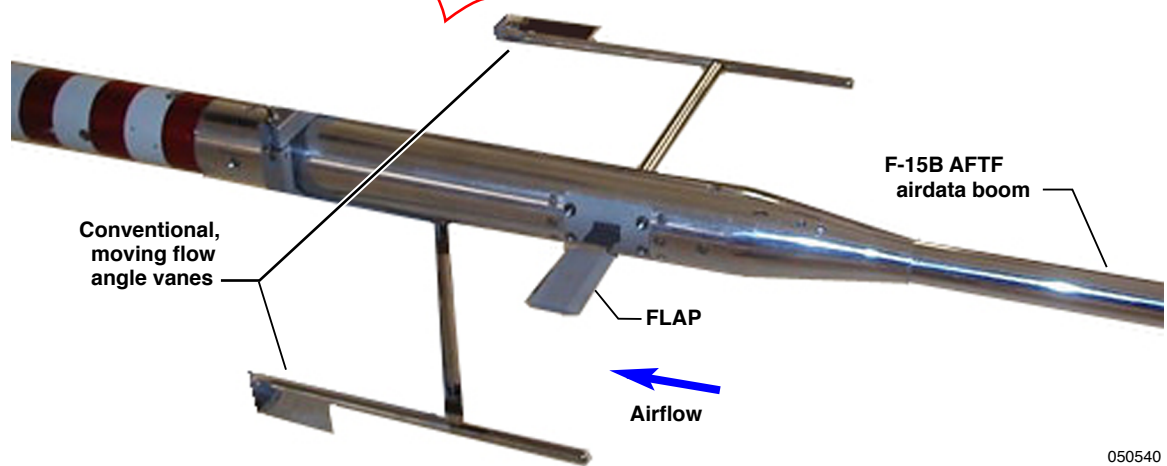
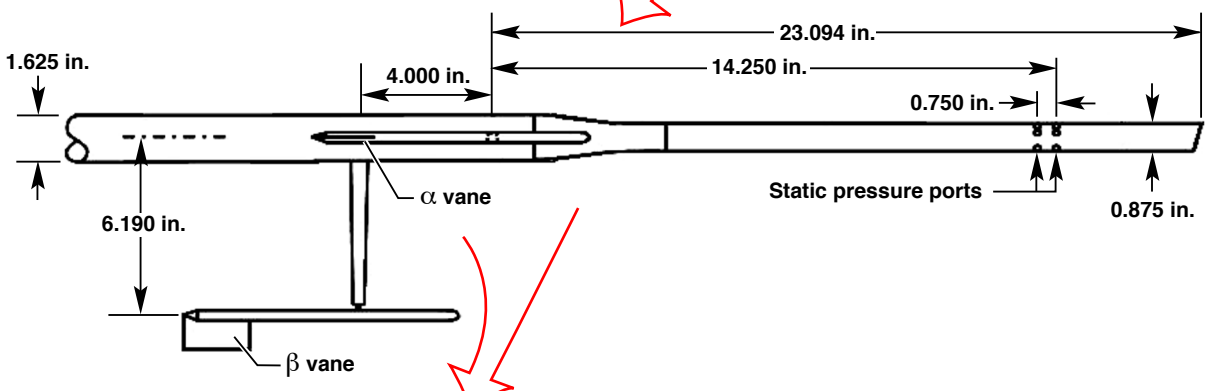
The FLAP is mounted on a NACA airdata boom located at the lower leading edge of the AFTF (fig. 12). Conventional moving vane probes for measuring angle of attack and angle of sideslip are also mounted on the airdata boom. The FLAP is mounted on the opposite side of the boom from the moving angle-of-attack vane. With this arrangement, the FLAP response could be directly compared with a conventional moving vane probe. Output wires from the FLAP strain gages are internally routed through the airdata boom into the AFTF.

Flight Test Conditions

Data were collected for the FLAP on ten F-15B flights. FLAP flight test data were collected at subsonic, transonic, and supersonic local flow Mach numbers to a maximum of 1.69. Data were obtained for various flight conditions including takeoff, landing, straight and level flight, flight at higher aircraft angles of attack, and flight at elevated *g*-loadings. Flight test maneuvers include angle-of-attack and angle-of-sideslip sweeps. Table 1 summarizes flight test results for the FLAP compared with a conventional moving vane probe. The flow conditions given in table 1 are the local flow conditions as measured upstream of the AFTF with the AFTF airdata boom.



EC00-0282-1



050540

Figure 12. Flow angle probe installed on F-15B Aerodynamic Flight Test Fixture airdata boom.

Table 1. Flow angle probe flight test results.

Flight number	Local flow conditions from AFTF airdata boom			FLAP	Moving vane	
	Pressure altitude, ft	Mach number	Dynamic pressure, psf	Angle of attack, deg	Angle of attack, deg	Angle of sideslip, deg
174	5,341	0.78	748	-3.2	-3.4	-0.4
174	5,332	0.70	603	-2.2	-3.2	-0.5
174	5,013	0.56	392	-2.3	-2.0	-0.1
174	3,883	0.51	337	-2.4	-2.3	-0.3
172	3,629	0.49	315	-2.8	-2.5	-0.5
171	3,834	0.53	367	-2.6	-2.8	-0.5
170	3,536	0.55	401	-2.8	-2.7	-0.2
169	3,894	0.53	356	-2.5	-2.7	-0.3
174	15,520	0.78	496	-2.5	-2.7	-0.2
174	15,194	0.59	290	-2.1	-2.0	-0.5
174	15,044	0.67	377	-1.8	-2.4	-0.2
174	14,961	0.70	407	-1.7	-2.5	-0.2
174	14,979	0.78	507	-2.6	-2.9	-0.2
174	15,407	0.91	676	-2.2	-3.1	-0.3
173	15,223	0.79	521	-2.9	-3.1	-0.5
173	15,262	0.91	681	-2.4	-3.2	-0.4
171	14,852	0.60	301	-1.9	-2.1	-0.5
171	14,838	0.79	531	-2.7	-3.0	-0.4
171	14,800	0.89	667	-2.3	-3.2	-0.4
169	15,081	0.60	299	-1.9	-2.1	0.0
169	15,157	0.70	410	-1.7	-2.7	-0.1
169	14,979	0.68	390	-1.5	-1.8	-0.1
169	15,368	0.70	405	-1.8	-2.7	-0.3
169	15,189	0.79	516	-2.8	-3.1	-0.3
169	15,485	0.91	674	-2.3	-3.3	-0.3
169	15,138	0.91	686	-2.1	-2.8	-0.2
174	29,924	0.78	270	-1.8	-2.1	-0.3
174	29,818	0.57	145	-0.3	-0.4	0.0
173	29,386	0.55	135	0.3	1.4	-0.7
173	29,709	0.58	153	-0.5	-0.7	-0.6
173	29,821	0.78	268	-1.7	-2.2	-0.4
173	29,251	0.99	443	-2.5	-2.5	-0.2
173	29,459	0.92	385	-1.9	-2.1	-0.3
173	29,669	1.07	516	-1.7	-1.7	-1.1
173	30,711	1.41	852	-4.3	-3.9	1.1
172	33,680	1.09	444	-1.8	-1.4	-0.9
172	33,787	0.80	235	-1.6	-2.2	-0.5

Table 1. Concluded.

Flight number	Local flow conditions from AFTF airdata boom			FLAP	Moving vane	
	Pressure altitude, ft	Mach number	Dynamic pressure, psf	Angle of attack, deg	Angle of attack, deg	Angle of sideslip, deg
172	33,766	1.11	455	-1.7	-1.8	-1.0
172	33,829	0.80	233	-1.6	-2.1	-0.5
172	33,752	1.10	449	-1.8	-1.7	-0.9
172	33,644	0.81	241	-1.7	-2.2	-0.5
172	33,554	1.11	459	-1.7	-1.8	-1.1
172	33,760	0.80	235	-1.7	-2.2	-0.6
172	33,691	1.11	454	-1.7	-1.8	-1.1
171	29,989	0.60	161	-0.4	-0.7	-0.6
171	29,892	0.80	285	-1.4	-2.1	-0.4
171	30,036	1.10	534	-1.6	-1.8	-1.1
170	29,838	1.37	829	-4.0	-3.6	1.2
169	29,769	0.58	150	-0.3	-0.7	0.1
169	29,868	0.69	211	-1.0	-1.7	0.0
169	29,903	0.78	269	-1.5	-2.2	-0.1
169	30,259	0.90	352	-1.9	-2.7	-0.3
169	29,924	1.07	510	-1.7	-1.6	-0.9
169	30,320	1.20	629	-2.4	-2.6	0.5
174	43,993	1.15	299	-1.4	-1.9	-0.6
174	44,370	0.98	213	-1.0	-1.6	0.1
174	44,271	0.85	160	0.4	-1.2	-0.1
174	44,445	0.77	130	0.4	-0.7	-0.3
173	43,762	1.34	412	-3.5	-3.1	1.1
173	43,456	1.05	258	-1.4	-0.8	-0.9
173	43,192	1.04	255	-1.4	-0.7	-0.8
173	44,603	0.78	133	0.1	-1.2	-0.6
172	39,196	1.69	813	-5.7	-6.3	1.0
172	44,650	0.93	191	-0.4	-1.4	-0.5
171	42,965	1.39	461	-3.4	-3.3	1.0
171	44,725	1.11	270	-1.2	-0.8	-0.7
171	45,027	0.81	142	0.2	-1.0	-0.6
170	44,690	1.38	421	-3.4	-3.1	1.2
170	44,519	1.10	268	-1.5	-0.6	-0.5
170	44,703	0.92	184	-0.7	-1.8	0.1
170	44,828	0.82	146	0.0	-1.0	0.1

RESULTS AND DISCUSSION

This paper compares flow angle flight test data obtained from the FLAP and from a conventional moving vane probe. This section discusses flow angle data comparisons as a function of Mach number and altitude, for level accelerations, and transonic flight. This section also presents results for angle-of-attack and angle-of-sideslip sweeps, higher aircraft angles of attack, wake turbulence, and g -load. For all of the data, the flow angle corresponds to the local angle of attack underneath the F-15B aircraft, upstream of the AFTF leading edge.

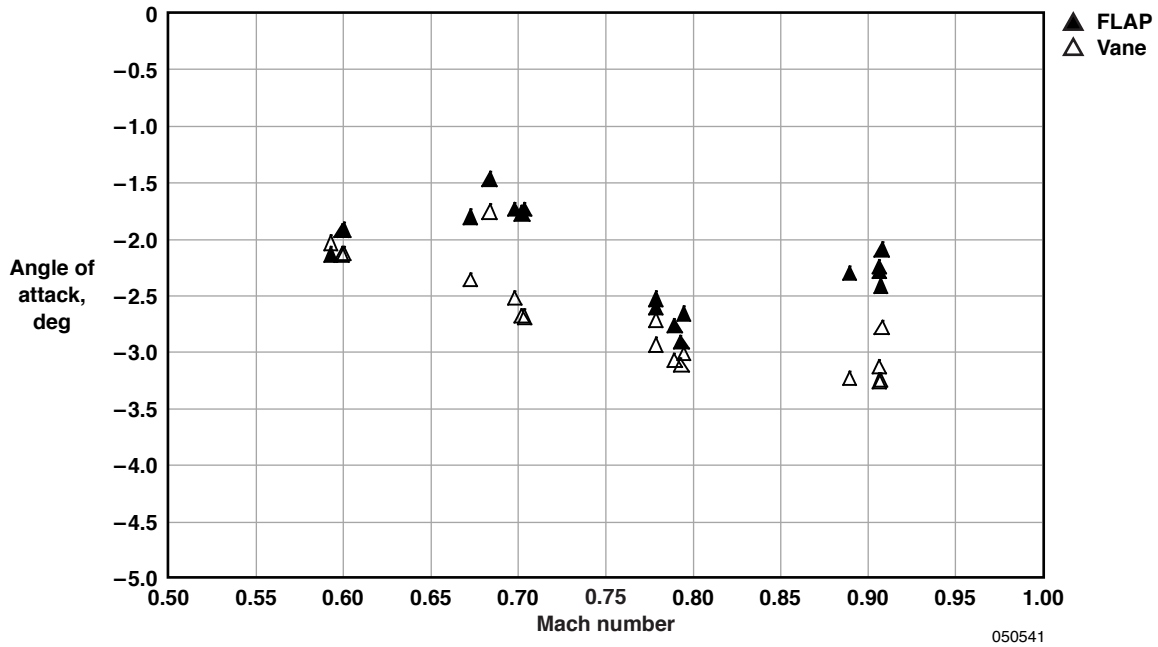
Results as Function of Mach Number and Altitude

Figure 13 compares the flow angle data obtained from the FLAP and from the conventional moving vane probe as a function of Mach number and altitude. Figures 13(a), 13(b), and 13(c) are for approximate pressure altitudes of 15,000 ft (4,572 m), 30,000 ft (9,144 m), and 45,000 ft (13,716 m), respectively. These data do not represent level accelerations at these discrete altitudes, but rather trimmed, unaccelerated flight at different Mach numbers within a few thousand feet of these altitudes. The Mach number is calculated from the static and total pressures measured at the AFTF airdata boom.

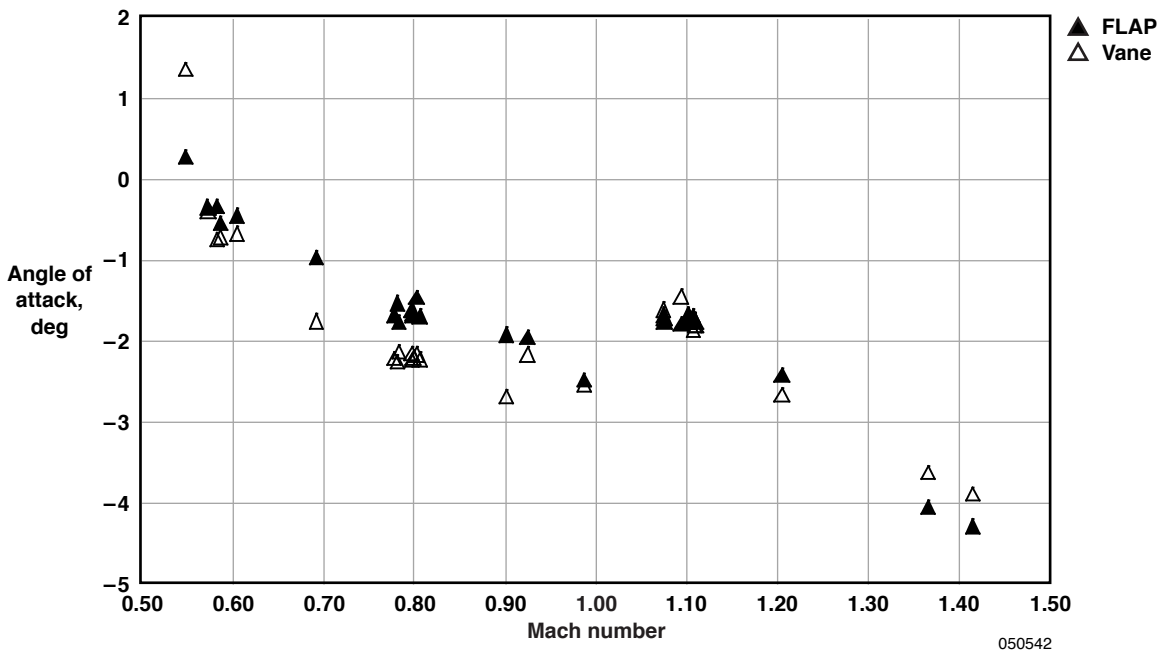
The data in figure 13(a) were obtained at altitudes between 14,800 ft (4,511.0 m) and 15,520 ft (4,730.5 m) and Mach numbers between 0.59 and 0.91. The data in figure 13(b) were obtained at altitudes between 29,250 ft (8,915.4 m) and 33,830 ft (10,311.0 m) and Mach numbers between 0.55 and 1.41. The data in figure 13(c) were obtained at altitudes between 39,200 ft (11,948 m) and 45,030 ft (13,725 m) and Mach numbers between 0.77 and 1.69.

For most Mach numbers, the local angle of attack is negative, indicating a local downwash underneath the aircraft, upstream of the AFTF. For higher altitudes, the aircraft flies at a slightly higher angle of attack resulting in less downwash and a smaller negative angle of attack at the AFTF. For example, at Mach 0.80, the AFTF angle of attack as measured with the moving vane is approximately -3.1 deg at 15,000 ft (4,572 m), approximately -2.2 deg at 30,000 ft (9,144 m), and approximately -1 deg at 45,000 ft (13,716 m). At 45,000 ft (13,716 m) altitude (fig. 13(c)), the FLAP-measured AFTF angle of attack varies from approximately $+0.1$ deg at Mach 0.80 to approximately -5.7 deg at Mach 1.70. The moving vane-measured angle of attack varies from approximately -1 deg at Mach 0.80 to approximately -5.8 deg at Mach 1.70.

At subsonic speeds, the FLAP angle of attack is a maximum of 1 deg less negative than indicated by the moving vane. At transonic speeds between Mach 1.00 and Mach 1.20, the FLAP angles of attack match the moving vane values at 30,000 ft (9,144 m) altitude and are a maximum of approximately 0.5 deg more negative than the moving vane at 45,000 ft (13,716 m). The FLAP and moving vane angles of attack are within 1 deg of each other at supersonic speeds above Mach 1.20.

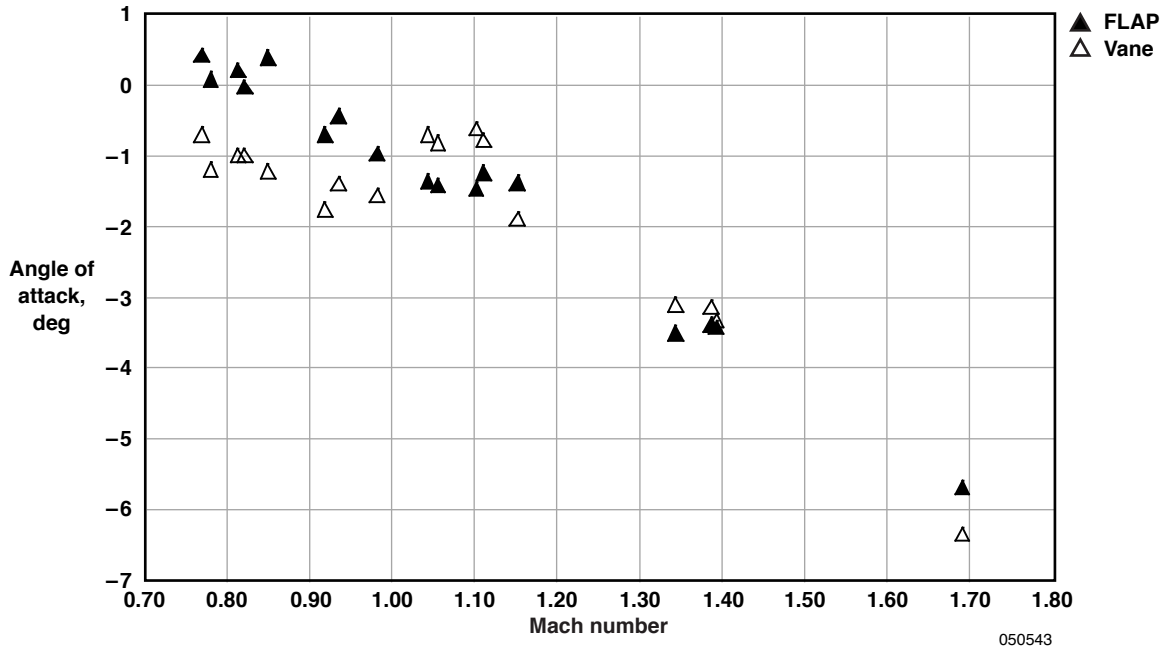


(a). At altitude of 15,000 ft (4,572 m).



(b). At altitude of 30,000 ft (9,144 m).

Figure 13. Flow angle probe and moving vane trim angle of attack compared with Mach number at several altitudes.



(c). At altitude of 45,000 ft (13,716 m).

Figure 13. Concluded.

Level Acceleration Results

Figure 14 shows angle of attack compared with time for a level acceleration from Mach 0.80 to Mach 1.70. Throughout the acceleration, the FLAP angle of attack closely matches the moving vane angle of attack except in the transonic region and more than Mach 1.50. The FLAP angle of attack varies from approximately -1.4 deg at Mach 0.80 to approximately -5 deg at Mach 1.70. The moving vane angle of attack varies from approximately -1.1 deg at Mach 0.80 to approximately -6.3 deg at Mach 1.70.

In the transonic region between Mach 0.98 and Mach 1.09, there is a step increase then decrease in the moving vane angle of attack, from approximately -1 deg to $+0.8$ deg, then back down to approximately -2 deg. The FLAP angle of attack decreases smoothly in this region, from approximately -1.3 deg to approximately -1.7 deg. The step increase may result from a localized shock wave that impinges on the moving vane, but not on the smaller profile of the FLAP.

Above Mach 1.50, the FLAP and moving vane data diverge, differing by approximately 1.3 deg at Mach 1.70. The FLAP angle of attack remains constant at -5 deg at Mach numbers ranging between 1.50 and 1.70. In this same Mach number range, the moving vane angle of attack decreases from approximately -5.6 deg to approximately -6.3 deg.

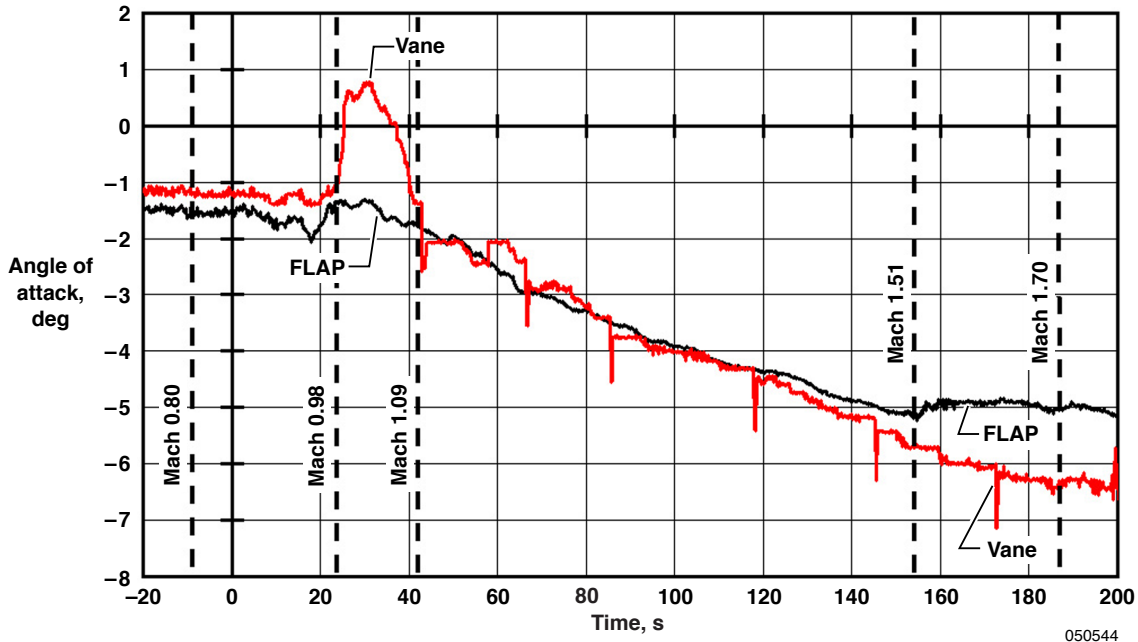


Figure 14. Comparison of flow angle probe and moving vane during level acceleration at altitude of 40,000 ft (12,192 m).

For the moving vane, there are six spike-like increases in the negative angle of attack during the acceleration, starting at Mach 1.09. During these “spikes,” the moving vane angle of attack increases in negative value by approximately 1 deg and then recovers to a slightly greater negative angle of attack than prior to the “spike.” The FLAP angle of attack is smooth and continuous throughout the same Mach number range. The cause of the “spikes” in the moving vane data is unknown. No anomalies in the instrumentation or data recording and telemetry systems could be found to explain this phenomenon.

Transonic Flight Results

Figure 15 shows transonic angle-of-attack data compared with time for acceleration from Mach 0.80 to Mach 1.10, followed by a deceleration to Mach 0.80. As seen previously in figure 14, there is a step change in the moving vane angle of attack in this region from approximately -2.5 deg to approximately -0.8 deg. The angle of attack then decreases and is constant at approximately -1.7 deg until Mach 1.10, when the angle of attack increases back to -0.8 deg. The step change in angle of attack may be a result of a transonic shock wave that is passing over or near the moving vane. The FLAP angle of attack increases, then decreases slightly and continuously over the acceleration or deceleration, from approximately -2.85 deg at Mach 0.80 to approximately -1.70 deg at Mach 1.10, then back to approximately -2.70 deg at Mach 0.80.

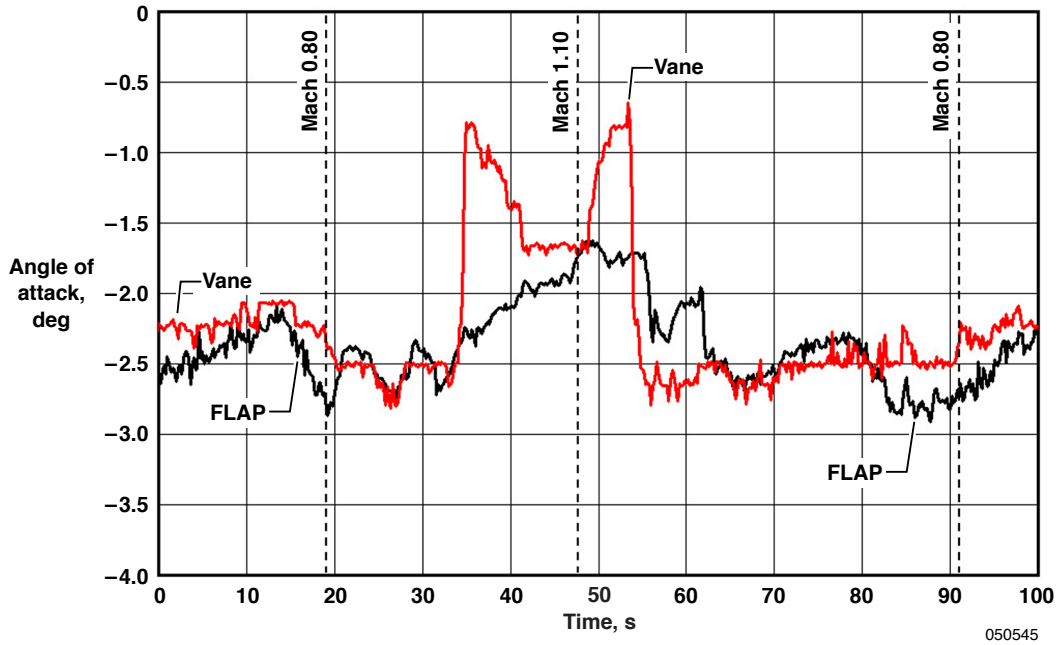


Figure 15. Comparison of flow angle probe and moving vane during transonic flight at altitude of 34,000 ft (10,363 m).

Response at High Aircraft Angles of Attack

Figure 16 compares measurements from the FLAP and the moving vane for the aircraft at high angles of attack. Data were obtained at subsonic Mach numbers and approximately 15,000 ft (4,572 m) altitude for aircraft angles of attack to a maximum of approximately 16.5 deg, as measured using the aircraft noseboom moving vane probes. The aircraft angle of attack varies from approximately +16.5 deg at Mach 0.30 to approximately +2 deg at Mach 0.66.

Both of the AFTF-mounted probes show a significantly lower local angle of attack under the aircraft. In this subsonic region between Mach 0.30 and Mach 0.67, the angles of attack obtained from the FLAP and moving vane are nearly identical. The moving vane angle of attack varies from approximately +5 deg at Mach 0.30 to approximately -2.5 deg at Mach 0.66. The FLAP angle of attack varies from approximately +4 deg to approximately -2 deg throughout the same Mach number range.

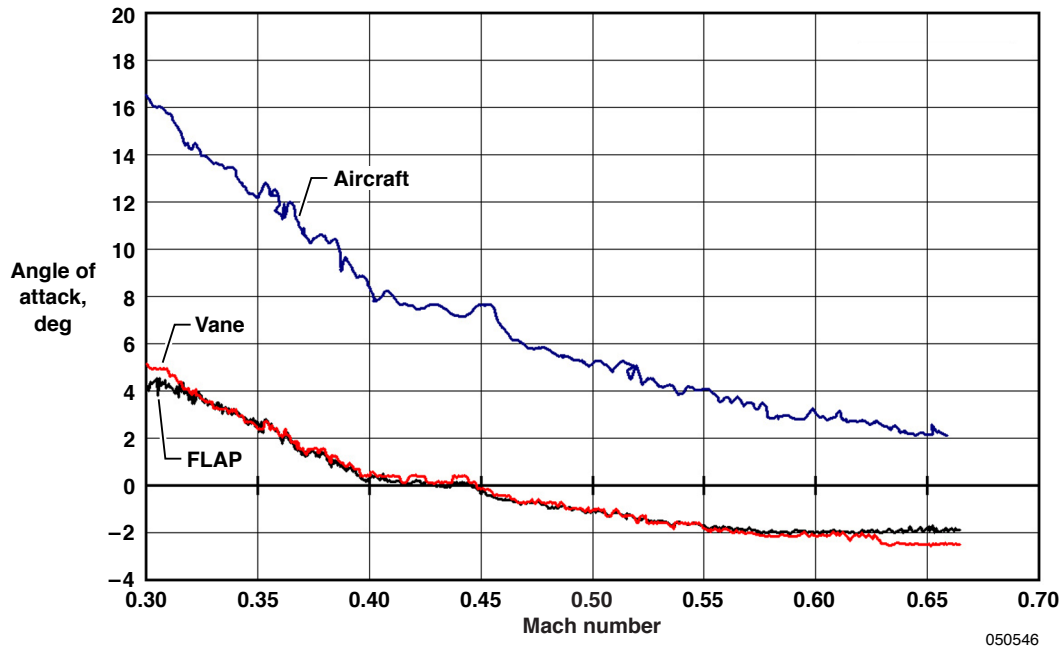


Figure 16. Comparison of flow angle probe and moving vane for higher aircraft angles of attack at altitude of 15,000 ft (4,572 m).

Angle-of-Attack Sweep Results

Figures 17(a) and 17(b) show data for angle-of-attack sweeps for subsonic and supersonic flight, respectively. These plots provide data on the transient response capability of the FLAP. Angle of attack is plotted compared with time for a pushover, pullup pitch sweep. Figure 17(a) shows an angle-of-attack sweep at Mach 0.80 at an altitude of 15,000 ft (4,572 m). Figure 17(b) shows an angle-of-attack sweep at Mach 1.40 at an altitude of 43,000 ft (13,106 m).

The FLAP and the moving vane have similar responses throughout the angle-of-attack sweep, although the peak magnitudes of the flow angle differ slightly. The largest difference is at supersonic speed where the FLAP indicates approximately a 0.25 deg less change in peak magnitude during the pullup portion of the maneuver. The subsonic sweep starts at approximately -3 deg angle of attack and varies from approximately -4 deg to approximately -1.1 deg. The supersonic sweep starts at approximately -3.4 deg angle of attack and varies from approximately -4 deg to approximately -2.2 deg and -2.4 deg for the moving vane and FLAP, respectively.

Effect of Sideslip

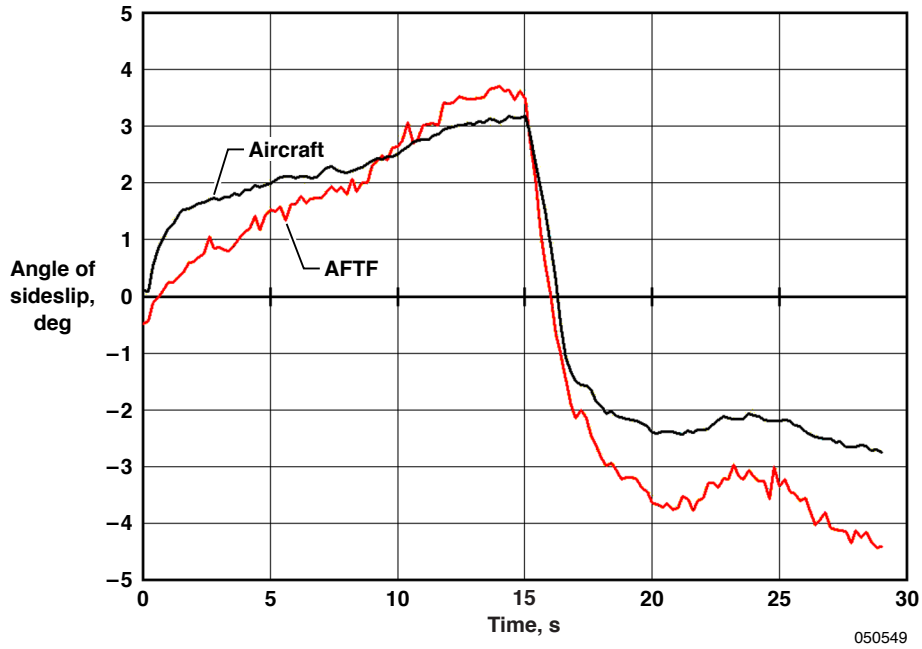
Figure 18 shows the effect of sideslip on the angle-of-attack probes at Mach 0.90 at an altitude of 15,400 ft (4,694 m). Figure 18(a) compares the aircraft and AFTF angle of sideslip. Recall that both angle-of-attack and angle-of-sideslip moving vanes were mounted on the AFTF airdata boom. The aircraft noseboom-measured sideslip varies from approximately +3.1 deg to approximately -2.7 deg. The local AFTF sideslip varies from approximately +3.6 deg to approximately -4.4 deg for the same maneuver.

Figure 18(b) shows the angle of attack measured by the FLAP, AFTF moving vane, and aircraft noseboom as a function of angle of sideslip. In discussing the sideslip data, recall that the moving vane probe and FLAP were mounted on the left and right sides of the AFTF airdata boom, respectively. At zero sideslip, the moving vane and FLAP angles of attack are approximately -3.3 deg and -2.2 deg, respectively, whereas the aircraft angle of attack is approximately 1 deg. The aircraft angle of attack is nearly constant at 1 deg during the sideslip maneuver. For positive sideslip (aircraft nose left), the FLAP and moving vane angles of attack stay constant at their respective zero sideslip values. For the maximum negative sideslip of -4.4 deg (aircraft nose right), the angle of attack decreases to approximately -3.6 deg and -3.1 deg for the moving vane and FLAP, respectively. Over the negative sideslip range, the FLAP-measured angle of attack changes by approximately 0.9 deg, from approximately -2.2 deg at zero sideslip to approximately -3.1 deg at -4.4 deg of sideslip. The moving vane measures a smaller change of approximately 0.3 deg over this sideslip range. The mounting location of each probe may influence the difference in the relative change from zero sideslip. The FLAP may be in the wake of the AFTF noseboom at negative sideslip, influencing its measured angle of attack.

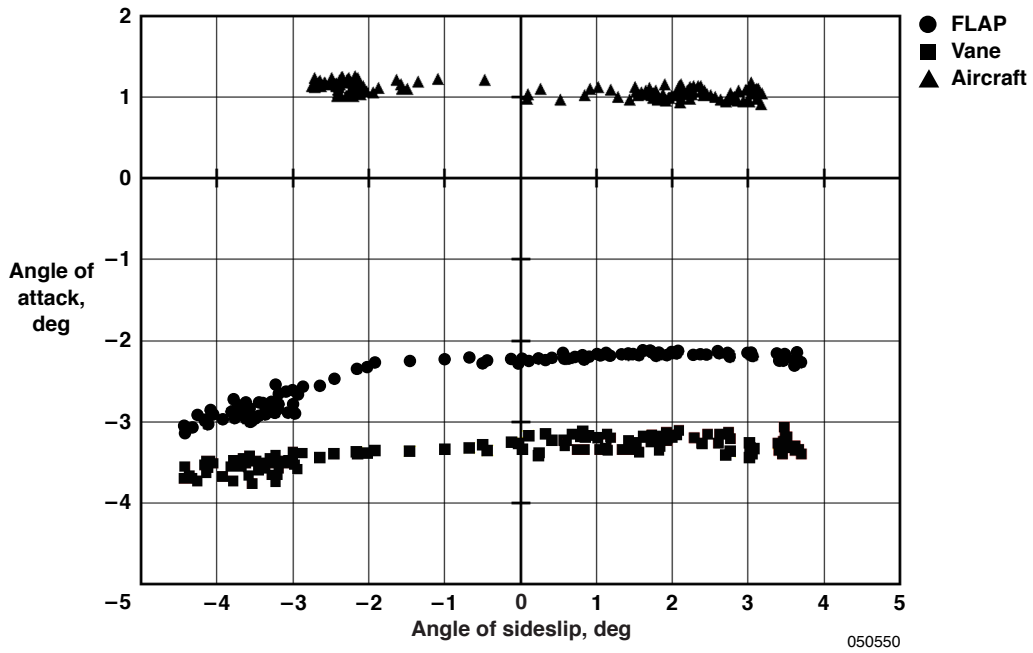
Response to Turbulence

In the landing gear down configuration, the wake from the aircraft nosewheel landing gear impinges on the AFTF airdata boom (ref. 12). This section compares the response of the FLAP and moving vane as a result of this wake turbulence.

Figures 19(a) and 19(b) show the response of the FLAP and moving vane, respectively, for an F-15B “touch-and-go” maneuver. Recall that the FLAP data were obtained at 16 times the sample rate as the moving vane (800 Hz compared with 50 Hz). The response of the moving vane may have an inherent lag and frequency limit associated with its mechanically rotating parts. The nonmoving FLAP does not have any mechanical lag and is limited only by the frequency with which the electronic signal from the strain gage bridge is obtained.

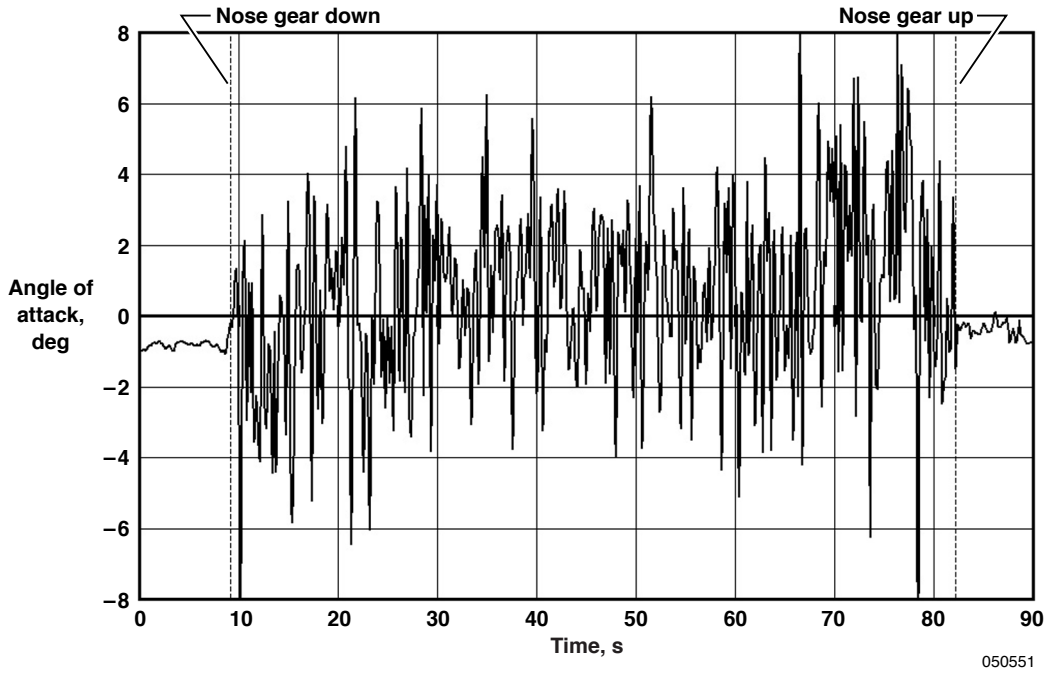


(a). Comparison of aircraft and Aerodynamic Flight Test Fixture angle of sideslip.

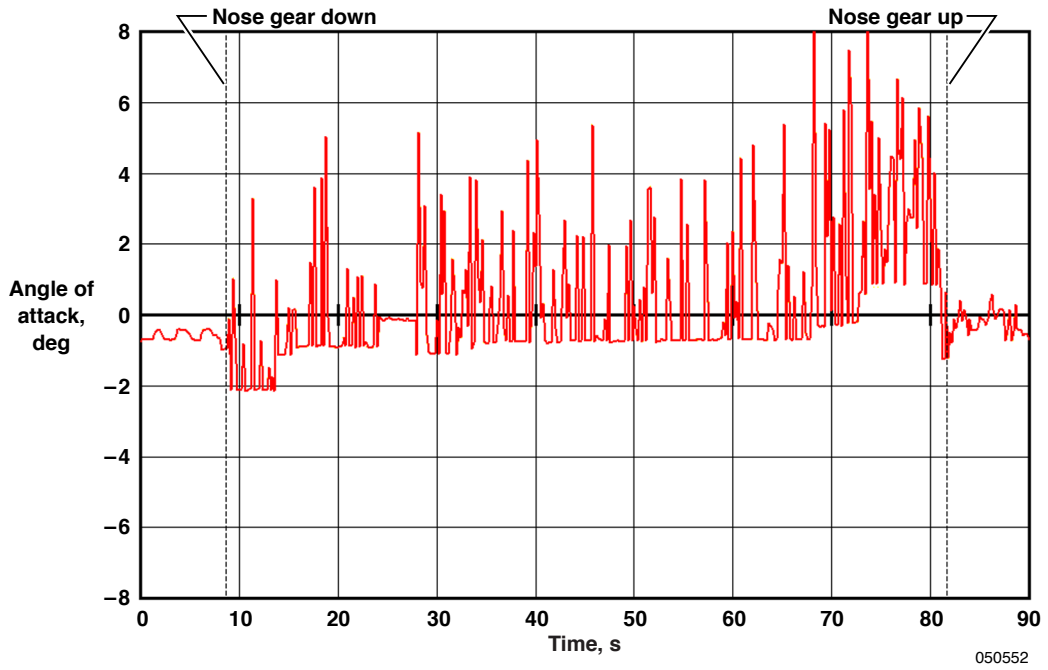


(b). Angle of attack measured as a function of angle of sideslip.

Figure 18. Effect of sideslip on the angle-of-attack probes at Mach 0.90 at altitude of 15,400 ft (4,694 m).



(a). Effect on flow angle probe.



(b). Effect on moving vane.

Figure 19. Effect of wake turbulence from nose landing gear.

The amplitude of the FLAP response is roughly ± 6 to ± 8 deg. The moving vane flow angle amplitude is similar to the FLAP for positive angles of attack, but is truncated at roughly -1 to -2 deg angle of attack. The cause of this truncation of the moving vane data is unknown, but association with the mechanical limitations of the rotating vane may affect this truncation.

Effect of g -Loading

Figure 20 shows the effect of normal acceleration on the FLAP. Plots from angles of attack from the FLAP and moving vane compare with normal acceleration or “ g -loading.” As expected, the angle of attack increases with increasing g -loading. For the moving vane, the angle of attack increases from approximately -2 deg at $1 g$ to approximately $+0.25$ deg at $2.25 g$. For the FLAP, the angle of attack increases from approximately -2 deg at $1 g$ to approximately -0.4 deg at $2.25 g$. In general, a higher angle of attack is obtained from the moving vane than the FLAP with increasing normal acceleration.

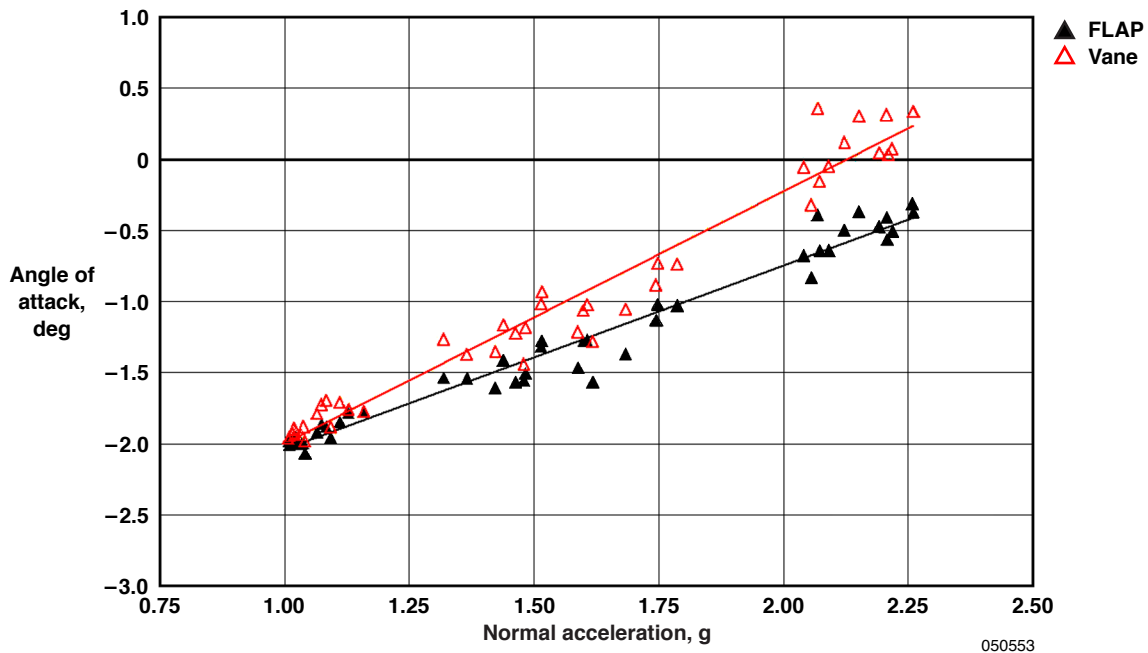


Figure 20. Effect of g -loading at Mach 0.50 at altitude range of 3,550 ft (1,082 m) to 3,950 ft (1,204 m).

FUTURE RESEARCH

The importance of future research is apparent. Future research to develop the force-based flow angle measurement technology may encompass the following areas:

- Plans include wind-tunnel calibration of the conventional strain gage-based FLAP. Starting with subsonic wind-tunnel tests, plans for FLAP calibrations include flow angles from 0 to 90 deg.
- Tests include different planform shapes for the FLAP in the wind tunnel and in flight. A smaller planform FLAP was designed and fabricated (fig. 21) for future wind-tunnel and flight testing.
- A fiber optic strain gage-based FLAP was designed and fabricated (fig. 21) for future flight testing using the original FLAP prototype planform. Fiber optic strain gage technology is used for the FLAP force measurement. Once validated on the original planform, the fiber optic-based FLAP could be significantly smaller in size than the conventional strain gage-based FLAP.

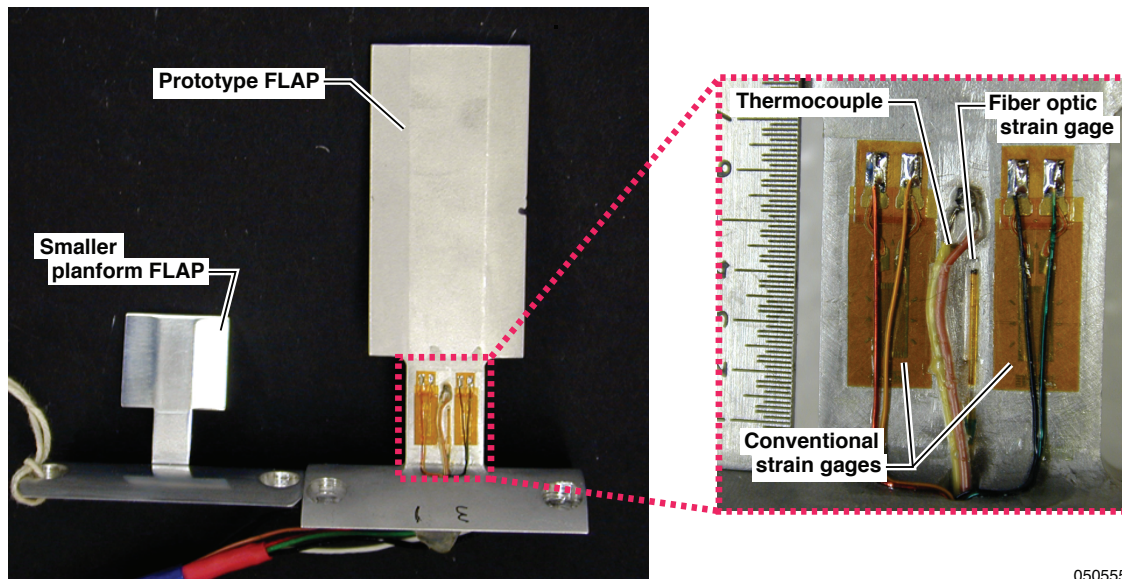


Figure 21. Future work includes fiber optic flow angle probe (right) and smaller planform flow angle probe (left).

CONCLUSIONS

The flow angle probe (FLAP) flight test results validated the feasibility of a force-based flow angle measurement probe. The angle-of-attack values obtained from the FLAP were compared with those obtained from a conventional moving vane probe. Although the FLAP flow angle calculation is based on a simple, two-dimensional flat plate analytical model, the flow angle measurements from the FLAP were in good agreement with those from the moving vane, both in terms of magnitude and trend, for many of the flight conditions and maneuvers tested. Requirements include further detailed calibrations to increase the accuracy of the FLAP flow angle measurement.

This paper reached significant conclusions for the various flight conditions and maneuvers. These conclusions encompass the following areas:

- The local angle of attack at the Aerodynamic Flight Test Fixture leading edge is negative for most flight Mach numbers, indicating a local downwash underneath the aircraft. For subsonic flight, the FLAP and moving vane angles of attack are in good agreement, differing by less than 1 deg. Below approximately Mach 0.60, the FLAP and moving vane values are nearly identical. At supersonic speeds more than Mach 1.10, the FLAP angle of attack is within 1 deg of the moving vane.
- During a level acceleration from approximately Mach 0.80 to Mach 1.70, the FLAP angle-of-attack matched the moving vane angle-of-attack values except at transonic speeds and more than Mach 1.50. At transonic speeds, the moving vane indicates discontinuous, stepwise changes in angle of attack. These step changes may indicate the impingement of a localized shock wave on the moving vane probe. The FLAP angle of attack varies smoothly in this transonic region, perhaps indicating insensitivity to this phenomenon. Above Mach 1.50, the FLAP and moving vane angles of attack diverge, differing by approximately 1.3 deg at Mach 1.70.
- At higher aircraft angles of attack to a maximum of approximately 16.5 deg, the FLAP and moving vane angles of attack are significantly lower than the aircraft values. Below approximately 8 deg aircraft angle of attack, the FLAP and moving vane angles of attack are the same.
- The FLAP matched the response of the moving vane throughout angle-of-attack sweeps at subsonic and supersonic flight conditions. The peak magnitude of the flow angle was approximately 0.25 deg lower for the FLAP than the moving vane at supersonic speed.

- The angle of attack measured as a function of sideslip was the same for the moving vanes on the Aerodynamic Flight Test Fixture and aircraft nosebooms. The FLAP angle of attack was a maximum of approximately 1 deg larger than the moving vane over the sideslip range. The angle-of-attack response because of sideslip may be influenced by the mounting location of each probe on the left or right side of the airdata boom.
- Angle-of-attack data were compared between the FLAP and moving vane for the turbulent flow caused by the wake flow from the nose landing gear. The moving vane response was truncated, perhaps a result of the inability of the rotating vane to respond at the frequency of the turbulent wake flow.
- Angle-of-attack data were obtained as a function of normal acceleration, to a maximum of approximately 2.25 g. A higher angle of attack was obtained from the moving vane than the FLAP with increasing normal acceleration.

*Dryden Flight Research Center
National Aeronautics and Space Administration
Edwards, California, October 24, 2005*

REFERENCES

1. Corda, Stephen and Michael Jake Vachon, *Airfoil Shaped Flow Angle Probe*, U.S. Patent No. 6,526,821 B1, 4 March 2003.
2. Richwine, David M., *F-15B/Flight Test Fixture II: A Test Bed for Flight Research*, NASA-TM-4782, 1996.
3. National Museum of Science and Technology, Milano, Italy, <http://www.museoscienza.org/english/leonardo/anemoscopio.htm>, Manuscript H3, folio 100 (43 v.) r., September 2005.
4. Wright, Orville and Wilbur Wright, *Flying-Machine*, U.S. Patent No. 1,075,533, 14 October 1913.
5. Mohler, S. R., “The “Automatic Stabilizer” and Angle of Attack Assessor: Human Factors Contributions of the Wright Brothers,” *Aviation, Space, and Environmental Medicine*, June 1996, Vol. 67, No. 6, pp. 585–8.
6. Tourmen, Louis, *Means for Detecting and Recording Water Wave Direction*, U.S. Patent No. 3,552,204, 5 January 1971.
7. Gerardi, Joseph J., *Omnidirectional Aerodynamic Sensor*, U.S. Patent No. 5,117,687, 2 June 1992.
8. Meyer, Robert R., Jr., *A Unique Flight Test Facility: Description and Results*, NASA TM-84900, 1982.
9. Corda, Stephen, M. Jake Vachon, Nathan Palumbo, Corey Diebler, Ting Tseng, Anthony Ginn, and David Richwine, *The F-15B Propulsion Flight Test Fixture: A New Flight Facility For Propulsion Research*, NASA/TM-2001-210395, 2001.
10. Palumbo, Nathan, Timothy R. Moes, and M. Jake Vachon, *Initial Flight Tests of the NASA F-15B Propulsion Flight Test Fixture*, NASA/TM-2002-210736, 2002.
11. Hoerner, Sigward F. and Henry V. Borst, *Fluid-Dynamic Lift*, Hoerner Fluid Dynamics, Albuquerque, NM, Second Edition, 1985.
12. Corda, Stephen, Russell J. Franz, James N. Blanton, M. Jake Vachon, and James B. DeBoer, *In-Flight Vibration Environment of the NASA F-15B Flight Test Fixture*, NASA/TM-2002-210719, 2002.

REPORT DOCUMENTATION PAGE				Form Approved OMB No. 0704-0188	
<p>The public reporting burden for this collection of information is estimated to average 1 hour per response, including the time for reviewing instructions, searching existing data sources, gathering and maintaining the data needed, and completing and reviewing the collection of information. Send comments regarding this burden estimate or any other aspect of this collection of information, including suggestions for reducing this burden, to Department of Defense, Washington Headquarters Services, Directorate for Information Operations and Reports (0704-0188), 1215 Jefferson Davis Highway, Suite 1204, Arlington, VA 22202-4302. Respondents should be aware that notwithstanding any other provision of law, no person shall be subject to any penalty for failing to comply with a collection of information if it does not display a currently valid OMB control number.</p> <p>PLEASE DO NOT RETURN YOUR FORM TO THE ABOVE ADDRESS.</p>					
1. REPORT DATE (DD-MM-YYYY) 28-02-2006		2. REPORT TYPE Technical Memorandum		3. DATES COVERED (From - To)	
4. TITLE AND SUBTITLE Design and Flight Evaluation of a New Force-Based Flow Angle Probe				5a. CONTRACT NUMBER	
				5b. GRANT NUMBER	
				5c. PROGRAM ELEMENT NUMBER	
6. AUTHOR(S) Stephen Corda and Michael Jacob Vachon				5d. PROJECT NUMBER	
				5e. TASK NUMBER	
				5f. WORK UNIT NUMBER 24-723-54-00	
7. PERFORMING ORGANIZATION NAME(S) AND ADDRESS(ES) NASA Dryden Flight Research Center P.O. Box 273 Edwards, CA 93523-0273				8. PERFORMING ORGANIZATION REPORT NUMBER H-2630	
9. SPONSORING/MONITORING AGENCY NAME(S) AND ADDRESS(ES) National Aeronautics and Space Administration Washington, DC 20546-0001				10. SPONSORING/MONITOR'S ACRONYM(S) NASA	
				11. SPONSORING/MONITORING REPORT NUMBER NASA/TM-2006-213673	
12. DISTRIBUTION/AVAILABILITY STATEMENT Unclassified - Unlimited Subject Category 02, 05, 07 Availability: NASA CASI (301) 621-0390 Distribution: Standard					
13. SUPPLEMENTARY NOTES					
14. ABSTRACT A novel force-based flow angle probe was designed and flight tested on the NASA F-15B Research Testbed aircraft at NASA Dryden Flight Research Center. The prototype flow angle probe is a small, aerodynamic fin that has no moving parts. Forces on the prototype flow angle probe are measured with strain gages and correlated with the local flow angle. The flow angle probe may provide greater simplicity, greater robustness, and better access to flow measurements in confined areas relative to conventional moving vane-type flow angle probes. Flight test data were obtained at subsonic, transonic, and supersonic Mach numbers to a maximum of Mach 1.70. Flight conditions included takeoff, landing, straight and level flight, flight at higher aircraft angles of attack and flight at elevated g-loadings. Flight test maneuvers included angle-of-attack and angle-of-sideslip sweeps. The flow angle probe-derived flow angles are compared with those obtained with a conventional moving vane probe. The flight tests validated the feasibility of a force-based flow angle measurement system.					
15. SUBJECT TERMS Aerodynamics, Airdata probes, Angle-of-attack probes, F-15B Flight testing, Flow angle measurement					
16. SECURITY CLASSIFICATION OF:			17. LIMITATION OF ABSTRACT	18. NUMBER OF PAGES	19a. NAME OF RESPONSIBLE PERSON
a. REPORT	b. ABSTRACT	c. THIS PAGE			STI Help Desk (e-mail: help@sti.nasa.gov)
U	U	U	UU	39	19b. TELEPHONE NUMBER (Include area code) (301) 621-0390